NEOPLASIA
www.neoplasia.com

Volume 16 Number 9 September 2014 pp. 723–740 723

Breast Cancer: Coordinated Regulation of CCL2 Secretion by Intracellular Glycosaminoglycans and Chemokine Motifs[1,2]

Yaeli Lebel-Haziv*, Tsipi Meshel*, Gali Soria*, Adva Yeheskel†, Elad Mamon* and Adit Ben-Baruch*

*Department of Cell Research and Immunology, George S. Wise Faculty of Life Sciences, Tel Aviv University, Tel Aviv, Israel; †Bioinformatics Unit, George S. Wise Faculty of Life Sciences, Tel Aviv University, Tel Aviv, Israel

Abstract

The chemokine CCL2 (MCP-1) has been identified as a prominent tumor-promoting factor in breast cancer. The major source for CCL2 is in the tumor cells; thus, identifying the mechanisms regulating CCL2 release by these cells may enable the future design of modalities inhibiting CCL2 secretion and consequently reduce tumorigenicity. Using cells deficient in expression of glycosaminoglycans (GAGs) and short hairpin RNAs reducing heparan sulfate (HS) and chondroitin sulfate (CS) expression, we found that intracellular HS and CS (= GAGs) partly controlled the trafficking of CCL2 from the Golgi toward secretion. Next, we determined the secretion levels of GFP-CCL2-WT and GFP-CCL2-variants mutated in GAG-binding domains and/or in the 40s loop of CCL2 (^{45}TIVA^{48}). We have identified partial roles for R18+K19, H66, and the ^{45}TIVA^{48} motif in regulating CCL2 secretion. We have also demonstrated that in the absence of R24 or R18+K19+^{45}TIVA^{48}, the secretion of CCL2 by breast tumor cells was almost abolished. Analyses of the intracellular localization of GFP-CCL2-mutants in the Golgi or the endoplasmic reticulum revealed particular intracellular processes in which these CCL2 sequences controlled its intracellular trafficking and secretion. The R24, ^{45}TIVA^{48} and R18+K19+^{45}TIVA^{48} domains controlled CCL2 secretion also in other cell types. We propose that targeting these chemokine regions may lead to reduced secretion of CCL2 by breast cancer cells (and potentially also by other malignant cells). Such a modality may limit tumor growth and metastasis, presumably without affecting general immune activities (as discussed below).

Neoplasia (2014) 16, 723–740

Introduction

Many recent studies provide evidence to the predominant roles played by inflammatory mediators in dictating the progression of malignant diseases. It is now generally accepted that inflammatory processes most commonly exert pro-tumorigenic effects and that the inflammatory microenvironment has major impact in promoting metastasis [1–4].

The inflammatory chemokine CCL2 (known also as MCP-1) is a prominent pro-cancerous inflammatory mediator, particularly in breast cancer [5–14]. The chemokine is expressed by leukocytes and stroma cells at the tumor site. However, the major source for CCL2 is in the breast cancer cells themselves, while it is hardly expressed by normal breast epithelial cells; moreover, in patients with breast cancer, high expression levels of CCL2 were correlated with advanced disease and early relapse [15–23]. Studies performed *in vivo* with animal model systems of breast cancer have modified the expression/activities of CCL2 or its CCR2b receptor and have indicated that this axis is directly and causatively responsible for breast tumor growth and dissemination of the cancer cells to distant organs [22–29].

As a member of the chemokine superfamily of leukocyte chemoattractants, CCL2 recruits myeloid cells and leads to high contents of tumor-associated macrophages (TAMs) and myeloid-derived suppressor cells in

Address all correspondence to: Adit Ben-Baruch, Head, Department of Cell Research and Immunology; Head, Ela Kodesz Institute for Research on Cancer Development and Progression, Department of Cell Research and Immunology, George S. Wise Faculty of Life Sciences, Tel Aviv University, Tel Aviv 69978, Israel. E-mail: aditbb@tauex.tau.ac.il

[1] This article refers to supplementary materials, which are designated by Figures W1 to W7 and Scheme W1 and are available online at www.neoplasia.com.

[2] This study was supported by the Federico Foundation.
Received 9 July 2014; Revised 11 August 2014; Accepted 12 August 2014

1476-5586/14
http://dx.doi.org/10.1016/j.neo.2014.08.004

breast tumors [20–25,30–32]. High abundance of TAMs in the tumors, together with the direct angiogenic activities of CCL2 on endothelial cells, contributes to the elevated angiogenic profile attributed to this chemokine [7,18,20,21,25,33–39]. In parallel, CCL2 promotes metastasis-related functions by acting directly on CCR2-expressing tumor cells, giving rise to tumor cell migration and invasion, to production of matrix metalloproteinases and to increased metastasis [14,22,23,26–29,40–43].

In the malignancy context, the "point of no return" is the step of CCL2 secretion, particularly from cancer cells, as they are the major source for the chemokine in breast tumors. Once released, the chemokine can induce all the above tumor-promoting functions by acting on cells of the tumor microenvironment and on the cancer cells. Inhibition of this crucial secretory step may halt many of the pro-tumoral activities of CCL2, and limit its ability to promote tumor growth and metastasis.

The aim of the current study was to identify intracellular components and chemokine motifs that regulate the secretion of CCL2 by breast tumor cells. Our published study indicated that in the chemokine CCL5, the 40s loop ^{43}TRKN^{46} sequence was absolutely required for the secretion of this chemokine by breast tumor cells and by other cell types as well [44]. In CCL5, the ^{43}TRKN^{46} motif is the sequence mediating the binding of the chemokine to extracellular glycosaminoglycans (GAGs) [45,46], a process required for leukocyte extravasation in inflamed tissues [47,48]. The GAG-binding capacity of ^{43}TRKN^{46} was found in our study to be relevant for processes of CCL5 secretion, as we could show that CCL5 release by breast tumor cells was partly mediated by intracellularly positioned GAGs [44]. Thus, CCL5 secretion was mediated by interactions between GAGs and the GAG-binding ^{43}TRKN^{46} motif, located in the 40s loop of the chemokine. Our research on the control of CCL5 secretion by its 40s loop and by GAGs has provided mechanistic views that extended previously published findings on the roles of the 40s loop in sorting of CXCL8 and CXCL4 to endothelial Weibel-Palade bodies and granules, respectively [49,50].

To follow on the above, we now asked the following questions: 1) Do intracellular GAGs regulate the secretion of CCL2? If so, which GAGs are involved in this process and to what extent do they affect it? 2) What are the CCL2 motifs that control its secretion? Does the process depend on GAG-binding domains of CCL2 and/or its 40s loop (=^{45}TIVA^{48})? Here, it is important to indicate that while CCL5 binds to GAGs mainly through the 40s loop, in CCL2 the situation is more complex: CCL2 binding to GAGs is mediated by several short amino acid (aa) sequences that are distributed along the chemokine, forming a GAG-binding sheet when quaternary structures are established by several CCL2 molecules [51,52].

The findings obtained in our current research identify the roles of intracellular GAGs and specific chemokine domains in regulating the intracellular trafficking and secretion of CCL2 by breast tumor cells. These observations open new opportunities for blocking the secretion of endogenous CCL2 by breast cancer cells and are thus of major clinical relevance in breast cancer and potentially also in other malignant diseases.

Materials and Methods

Cell Cultures

Human breast adenocarcinoma MDA-MB-231 cells were grown in Dulbecco's modified Eagle's medium (DMEM) supplemented with 10% fetal calf serum, 2 mM L-glutamine, 100 units/ml penicillin, 100 μg/ml streptomycin, and 250 ng/ml amphotericin (all purchased from Biological Industries, Beit Haemek, Israel). In this study, we used two spontaneous variants of MDA-MB-231 cells, expressing either low or high levels of endogenous CCL2 [22,27,40,41,53] (the latter cells were kindly provided by Dr Gilles, University of Liège, Liège, Belgium). Human embryonic kidney–293 (HEK 293) cells were maintained in DMEM as above. Chinese hamster ovary (CHO) cells were also used in the study (kindly provided by Prof. Vlodavsky, Technion, Haifa, Israel): CHO-K1 and CHO-pgsA-745 cells were cultured in DMEM and Roswell Park Memorial Institute (RPMI) medium, respectively, supplemented as above [with the addition of 1 mM sodium pyruvate (Biological Industries)]. Before different experimental procedures, the various cell lines were transferred to their corresponding serum-free media, except for HEK 293 cells that were continuously grown in their serum-including medium.

Table 1. The aa Composition of GFP-CCL2 WT and GFP-CCL2 Mutants Used in the Study.

Chemokine	Sequence
GFP-CCL2-WT	N'–FTN<u>RK</u>ISVQ<u>R</u>LA...AVIFK<u>TIVA</u>KE... VQDSMD<u>H</u>LD…-GFP 15 1819 24 45 48 66
GFP-CCL2-R18A+K19A	N'–FTN<u>AA</u>ISVQRLA...AVIFKTIVAKE... VQDSMDHLD…-GFP 15 1819 24 45 48 66
GFP-CCL2-R24A	N' –FTNRKISVQ<u>A</u>LA...AVIFKTIVAKE... VQDSMDHLD…-GFP 15 1819 24 45 48 66
GFP-CCL2-H66A	N'–FTNRKISVQRLA...AVIFKTIVAKE... VQDSMD<u>A</u>LD…-GFP 15 1819 24 45 48 66
GFP-CCL2-TIVA--	N' –FTNRKISVQRLA...AVIFK<u>AAAA</u>KE... VQDSMDHLD…-GFP 15 1819 24 45 48 66
GFP-CCL2-R18A+K19A+TIVA--	N' –FTN<u>AA</u>ISVQRLA...AVIFK<u>AAAA</u>KE... VQDSMDHLD…-GFP 15 1819 24 45 48 66

The table denotes sequences of CCL2 WT and its mutated variants. Bold and underlined, sequences that were mutated in each CCL2 variant compared to the WT chemokine. The numbers indicate the position of the amino acids in the mature CCL2 protein. N′, amino terminus of CCL2.

Chemokine Sequences

The vector used in the analyses of this study was pEGFP-N1, designed to express wild type (WT) or mutated CCL2 (Table 1). The constructs of WT and mutated CCL2 were produced by polymerase chain reaction, and the sequences of all chemokines (WT and mutated) were validated by full-length sequencing.

Bioinformatics Analyses of CCL2 Mutants

To predict the appropriate folding of mutated CCL2 proteins, an *ab initio* protocol was applied, which predicts the structure of a protein based on its sequence. Models were built using Rosetta 3.1 AbinitioRelax protocol, with protein structure prediction using Rosetta [54]. The final models presented were chosen out of 10,000 decoys, based on their lowest score. The models were further assessed using the MolProbity web server [55]. The model structures of CCL2 mutants (Table 1) were superimposed on the published X-ray structure of CCL2-WT (PDB 1DOK [56]). Positions 1 to 13 were not shown in the relevant figures because the mutated chemokines were modeled as monomers, whereas the published X-ray structure of CCL2-WT was of a dimer, in which the N′ is differently organized compared to the monomer. Positions 70 to 76 were not shown because no coordinates were available in the X-ray structure of CCL2-WT.

Transfection by GFP-CCL2 Constructs and Determination of Transfection Yields

The different cell types were transiently transfected with constructs of GFP-CCL2 WT or GFP-CCL2-mutants (Table 1) using MP-100 MicroPorator (Digital Bio, Seoul, Korea; according to the manufacturer's instructions) or by ICAFectin TM 441 DNA transfection

reagent (Cat. No. ICA441; In-Cell-Art, Nantes, France; according to the manufacturer's instructions). Transfection outcome was evaluated by flow cytometry analyses (FACS). To this end, the cells were washed with phosphate-buffered saline supplemented with 0.02% sodium azide, and the expression of GFP was determined with a Becton Dickinson FACSort (Mountain View, CA) using the CellQuest software.

Down-Regulation of Heparan Sulfate and Chondroitin Sulfate Expression by Short Hairpin RNAs Targeting Exostosin Glycosyltransferase or Chondroitin Sulfate Synthase

Heparan sulfate (HS) and chondroitin sulfate (CS) are saccharides; thus, they could not be downregulated directly by short hairpin RNAs (shRNAs) but rather by targeting key enzymes involved in their synthesis, namely, exostosin glycosyltransferase (EXT) and chondroitin sulfate synthase (CHSY), respectively. Down-regulation of EXT or CHSY expression was performed by lentiviral infection with shRNA. Several different shRNAs were assayed and the most effective ones were chosen for use throughout the study. In the case of EXT, down-regulation of EXT2 was performed by a combination of two different shRNA clones (both from Sigma-Aldrich, Rehovot, Israel): 1) Cat. No. SHCLNG-NM_000401.1-2839s1c1 and 2) Cat. No. SHCLNG-NM_000401.x-2366s1c1. In the case of CHSY, down-regulation of CHSY1 was assumed by shRNA Cat. No. SHCLNG-NM_014918.3-1964s1c1 (Sigma-Aldrich). Following infection, selection was performed with 4 μg/ml puromycin (A.G. Scientific, San Diego, CA). Then, the cell population was used as a whole to prevent bias toward specific cell clones. Control cells were infected with control shRNA vectors (Sigma-Aldrich) carrying similar antibiotic resistance. Down-regulation of EXT2 or CHSY1 was verified by reduced expression of HS or CS in the cells, using confocal analyses (please see below).

Determination of CCL2 Secretion by enzyme-linked immunosorbent assay (ELISA)

Different cell types have undergone transfection or infection as described above and then were grown in serum-free medium for 24 to 48 hours (except for HEK 293 cells, as mentioned above). In specific experiments, MDA-MB-231 cells were treated with brefeldin A (BFA; 5–10 μg/ml; Cat. No. B7651; Sigma-Aldrich) for 2 hours at 37°C before ELISAs. BFA did not affect cell viability.

In all cases, human CCL2 levels in cell conditioned medium were determined by ELISA using standard curves with rhCCL2 (Cat. No. 300-04; PeproTech, Rehovot, Israel), at the linear range of absorbance. The following antibodies were used (all from PeproTech): coating rabbit polyclonal antibodies (Cat. No. 500-p34); detecting biotinylated rabbit polyclonal antibodies (Cat. No. 500-P34Bt). After the addition of streptavidin-horseradish peroxidase (HRP; Cat. No. 016-030-084; Jackson ImmunoResearch Laboratories, West Grove, PA), the substrate TMB/E solution (Chemicon, Temecula, CA) was added. The reaction was stopped by the addition of 0.18 M H_2SO_4 and the absorption was measured at 450 nm. In parallel, cells were removed by trypsinization and counted by trypan blue exclusion (Cat. No. 03-102-1B; Biological industries), and the ELISA results were presented as ng/10^7 cells.

Determination of CCL2 Expression by Western Blot Analysis

MDA-MB-231 cells were transiently transfected with constructs of GFP-CCL2 WT, GFP-CCL2 mutants, or control GFP vector. Cells were lysed in RIPA lysis buffer and immunoprecipitation was performed with mouse monoclonal IgG antibody against GFP (Cat. No. M048-3; Covance, Princeton, NJ; MBL International, Woburn, MA). Immunoprecipitation was followed by conventional Western blot (WB) procedure, using rabbit IgG polyclonal antibodies against human CCL2 (Cat. No. 500-p34; PeproTech). HRP-conjugated goat anti-rabbit IgG antibodies (Cat. No. 111-035-003; Jackson ImmunoResearch Laboratories) were used as secondary antibodies. In parallel, blots were reacted with mouse monoclonal IgG antibodies against GFP and then with secondary goat anti-mouse antibodies (Cat. No. 115-035-166; Jackson ImmunoResearch Laboratories. Data not shown). The membranes were subjected to enhanced chemiluminescence.

Confocal Analyses

Endogenous CCL2 was detected in the cells by staining with monoclonal IgG antibodies against human CCL2 (Cat. No. 500-M71; PeproTech) and then with fluorescein isothiocyanate–conjugated goat anti-mouse IgG antibodies (Cat. No. 115-095-003; Jackson ImmunoResearch Laboratories).

In experiments using GFP-CCL2 constructs (WT or mutated), the transfected cells were grown in growth medium on coverslips for 24 hours and then in serum-free medium for another 24 hours at 37°C. Cells were fixed with 8% paraformaldehyde (Cat. No. 1.04005; Merck KGaA, Darmstadt, Germany), permeabilized by 0.2% Triton (Cat. No. X-100; Sigma-Aldrich), and blocked with 2% BSA (Cat. No. 0332-TAM; Amresco, Solon, OH). To determine the localization of GFP-CCL2 WT or GFP-CCL2 mutants in the Golgi, a vector expressing the Golgi marker α-mannosidase IB, tagged by hemagglutinin (HA), was expressed by transfection in the cells. HA was detected by rabbit IgG antibodies against HA (Cat. No. sc-805; Santa Cruz Biotechnology, Santa Cruz, CA) and then with DyLightTM 549–conjugated AffiniPure goat anti-rabbit IgG antibodies (Cat. No. 111-505-144; Jackson ImmunoResearch Laboratories). To determine the localization of GFP-CCL2 WT or GFP-CCL2 mutants in the endoplasmic reticulum (ER), staining was performed with rabbit IgG antibodies against calnexin (Cat. No. sc-11397; Santa Cruz Biotechnology) and then with DyLightTM 549–conjugated AffiniPure goat anti-rabbit IgG antibodies (as above). Quantification of co-localization of GFP-CCL2 WT or GFP-CCL2 mutants with markers of the Golgi or the ER was performed by Slidebook TM or ImageJ software, respectively, applied on a large number of cells.

In parallel, experiments were performed to determine the co-localization of GFP-CCL2 WT with GAGs (HS and CS) in the Golgi. In these experiments, MDA-MB-231 cells were transiently transfected by a construct expressing GFP-CCL2 WT and simultaneously with a vector expressing the Golgi marker α-mannosidase IB, tagged by HA. The cells were stained with rabbit IgG antibodies against HA (as above), followed by DyLightTM 549–conjugated AffiniPure goat anti-rabbit IgG antibodies (as above) and with mouse IgM antibodies against HS or CS (HS: Cat. No. 370255; SEIKAGAKU Corporation, Tokyo, Japan; CS: Cat. No. c-8035; Sigma-Aldrich), followed by Alexa Fluor 647 goat anti-mouse IgM antibodies (Cat. No. A-21238; Invitrogen, Carlsbad, CA).

To examine the expression levels of HS and CS in MDA-MB-231 cells that were stably infected with EXT2 shRNAs or CHSY1 shRNA or in CHO cells, the cells were stained with mouse IgM antibodies against HS or CS, followed by Alexa Fluor 647 goat anti-mouse IgM antibodies, as above.

In all the experiments, negative controls included cell staining by isotype-matched non-relevant antibodies, followed by secondary antibodies, as appropriate (data not shown). Coverslips were mounted

using fluorescent mounting medium (Cat. No. E18-18; Golden Bridge International, Mukilteo, WA) and read by ZEISS LSM-510 confocal microscopy.

Statistical Analyses and Data Presentation

Statistical analyses were done using Student's *t* tests. Values of $P < .05$ were considered statistically significant. Adjustment for multiplicity of comparisons was done using the Benjamini-Hochberg procedure. Using this procedure, all the significant results that were presented in the manuscript remained statistically significant after correcting for their multiplicity. Each type of ELISA experiment was repeated at least three independent times with reproducible results and the findings were presented as a representative experiment of these similar repeats (except for BFA results, because of technical reasons). The confocal pictures are representatives of many pictures that were taken in at least three independent experiments and their quantitative results were presented as mean ± standard deviation (SD) of values obtained from many pictures.

Results

The Trafficking of CCL2 from the Golgi toward Secretion Partly Depends on Intracellular GAGs

In this study, our aim was to determine the mechanisms regulating the secretion of CCL2 by breast tumor cells. To this end, we used a cell system that is conventionally used in breast cancer studies, based on MDA-MB-231 breast tumor cells. Two spontaneous variants of MDA-MB-231 have been described in the literature, one expressing endogenously low levels of CCL2 (to be called herein "MDA-CCL2-low" cells [22,27,53]) and the second expressing high levels of the chemokine ("MDA-CCL2-high" cells [40,41]). In our study, the use of such two variant cell lines has enabled us to optimally address different aspects of the study, as follows: 1) MDA-CCL2-low cells—These cells provided an excellent platform for clearly comparing the secretion properties of different CCL2 variants by overexpressing GFP-CCL2 WT or GFP-CCL2 mutants. In addition, using the GFP signal as readout, we could decipher the localization of CCL2 WT and of GFP-CCL2 mutants in the Golgi and ER, with high-quality confocal analyses. 2) MDA-CCL2-high cells—With these cells, we could identify in great detail the mechanisms regulating the secretion of endogenous CCL2 by using pharmacological inhibitors or shRNAs.

To establish the MDA-CCL2-low–based system in our study, the cells have undergone transfection by a GFP-CCL2 WT construct (Figure W1*A*1; GFP expressed at the carboxyl terminus of the molecule; Table 1), leading to productive secretion of the chemokine by the cells (Figure W1*A*2). Following overexpression of GFP-CCL2 WT, the levels of CCL2 WT in cell supernatants were generally at the range of ~ 80 to 500 ng/10^7 cells, depending on transfection yields. These CCL2 levels agreed well with the levels of CCL2 generally produced endogenously by MDA-CCL2-high cells (see below). GFP-CCL2 WT has gained a vesicular phenotype in the MDA-CCL2-low cells transfected by the construct (Figure W1*B*1), which was similar to the phenotype of endogenous CCL2 in MDA-CCL2-high cells (Figure W1*B*2). In both cell types—MDA-CCL2-low cells transfected by GFP-CCL2 WT and MDA-CCL2-high cells—CCL2 had a vesicular distribution and a typical Golgi localization (as will be shown later by more specific analyses), standing in line with the secretory nature of the chemokine.

To identify the intracellular path taken by CCL2 WT on its way toward secretion, we first determined the co-localization of transfected GFP-CCL2 WT with Golgi or ER markers in the transfected MDA-CCL2-low cells. Definite positioning of the chemokine in the Golgi was identified by substantial co-localization of GFP-CCL2 WT with the Golgi marker α-mannosidase IB (Figure 1*A*) and relatively limited co-localization with the ER marker calnexin (Figure 1*B*). These results suggested that CCL2 WT takes the ER-to-Golgi route in its way toward secretion, as do many secreted proteins. Indeed, specific inhibition of ER-to-Golgi trafficking by BFA in MDA-CCL2-high cells has led to substantial reduction, of 70.9 ± 15.2% in CCL2 secretion in the different experiments, indicating that the chemokine takes the ER-to-Golgi route toward secretion (Figure 1*C*).

To determine the roles of intracellular GAGs in the secretion of CCL2 WT, we first asked whether the chemokine was co-localized with GAGs intracellularly. Published reports indicated that HS and CS are the two most abundant GAGs expressed by MDA-MB-231 cells and that the two GAGs share the ability to bind CCL2 [57–59]. In our analyses of GFP-CCL2 WT in transfected MDA-CCL2-low tumor cells, we found that CCL2 was highly co-localized with HS and with CS (Figure 2, *A* and *B*, respectively). In parallel, we found preferential expression of HS and CS in the Golgi; consequently, definite co-localization of GFP-CCL2 WT with HS and CS in the Golgi has been revealed (Figure 2, *A* and *B*, respectively). Taken together, all of the above findings indicate that CCL2 WT exits the ER and reaches the Golgi. The results also suggest that CCL2 associates with GAGs in the Golgi and then proceeds toward secretion.

To further address the involvement of GAGs in CCL2 secretion, we have taken advantage of the well-studied CHO cell system consisting of variants selected for mutations in GAG expression [60]. Specifically, in this study, we used 1) CHO cells expressing normal levels of GAGs, originally termed CHO-K1, which for the sake of clarity were given the name CHO-GAG+++ in our current study, and 2) CHO cells that are almost completely deficient in expression of all GAGs due to substantial reduction in the expression of xylosyltransferase, the enzyme that initiates the process of GAG synthesis [61]. In the past, it was shown that these latter CHO-deficient GAG cells (originally termed CHO-pgsA-745) did not have a general defect in secretion [62]. In line with the original characterization of these two cell lines in the literature, we found that the CHO-deficient GAG cells exhibited almost complete inhibition in expression of HS and CS (Figure W2*A*).

Using the CHO cell–based system, we asked whether deficiency in GAG expression would affect the intracellular localization and secretion of CCL2. Because GAGs are synthesized mainly in the Golgi [63–65], we expected that the ER-to-Golgi step will not depend on GAGs, and thus, the levels of CCL2 localization in the Golgi will be similar in CHO-GAG+++ cells and in CHO-deficient GAG cells. Indeed, following the expression of GFP-CCL2 WT (Figure W2*B*), the extent of CCL2 positioning in the Golgi was similar in the two cell types (Figure 3, *A*–*C*). However, in the absence of GAGs, the secretion of CCL2 WT was partly and significantly inhibited (Figure 3*D*), showing an average of 59.4 ± 16.2% reduction in CCL2 WT secretion in the different experiments. Taken together, these results indicate that GAGs partly regulate the process of CCL2 secretion and suggest that GAGs control the intracellular trafficking of CCL2 at the post-Golgi stage.

HS and CS Partly Mediate the Process of CCL2 Secretion by Breast Tumor Cells

The above findings, demonstrating that the secretion of CCL2 WT required partial involvement of GAGs, led us to ask if the secretion of

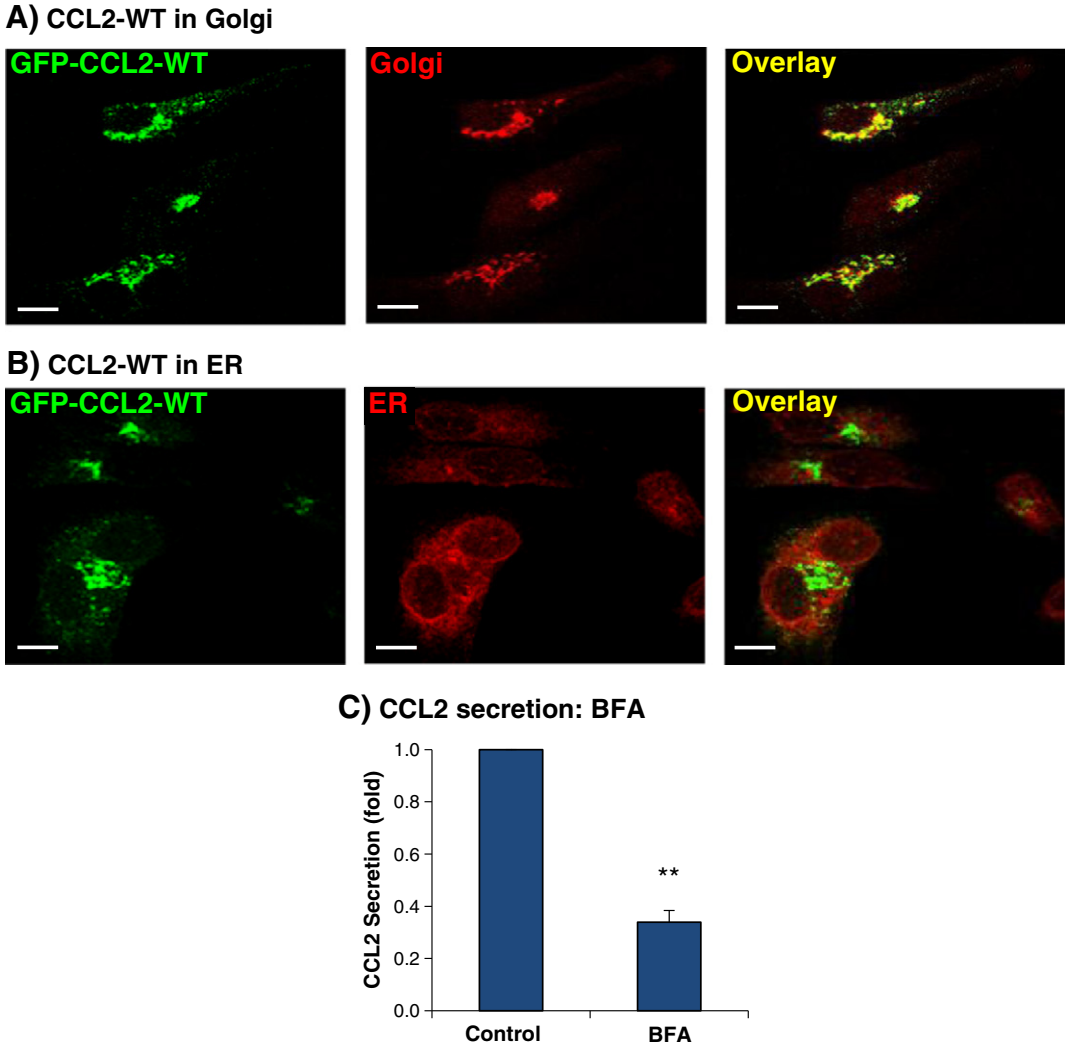

Figure 1. CCL2 WT takes the ER-to-Golgi route toward secretion. MDA-CCL2-low cells were transfected to express GFP-CCL2 WT. Additional characteristics of the transfected cells are shown in Figure W1. (A and B) After 48 hours, the intracellular localization of CCL2 was determined by confocal analyses of the GFP signal. (A) GFP-CCL2 WT expression in the Golgi. In parallel to expression of GFP-CCL2 WT, the expression of the Golgi marker α-mannosidase IB was determined by antibodies. (B) GFP-CCL2 WT expression in the ER. In parallel to expression of GFP-CCL2 WT, the expression of the ER marker calnexin was determined by antibodies. In A and B, negative controls included staining by non-relevant isotype-matched antibodies (data not shown). The results are representatives of many pictures that were taken in $n > 3$ independent experiments. Bar, 10 μm. (C) The secretion of CCL2 required for ER-to-Golgi transport of the chemokine. The cells were treated by BFA (5-10 μg/ml; 2 hours), and the levels of CCL2 in cell supernatants were determined by sandwich ELISAs, at the linear range of absorbance. Untreated cells (control) were given the value of 1. C presents normalized results of a representative experiment of $n > 3$ independent experiments, where $^{**}P < .01$ comparing between BFA-treated and untreated cells. The P value was calculated from the original test values, before normalization. Inhibition levels by BFA were 70.9 ± 15.2% in the different experiments.

CCL2 will be reduced in breast cancer cells that do not express HS and CS. To generate such cells, we chose to take the shRNA approach. Because HS and CS are saccharides, we could not target them directly but rather had to target key enzymes that synthesize them. Thus, as a general outline, we expressed in MDA-CCL2-high cells different shRNAs that targeted HS- or CS-generating enzymes. The relevant readout in this part of the study was extensive and marked inhibition of the actual expression of HS or CS in the cells, analyzed by the most appropriate tool of specific antibodies directed to HS and CS (as saccharides, the GAGs could not be analyzed at the mRNA level; WB studies were expected to be problematic because of the relative low binding affinity of GAGs to proteins). Following the infection of the cells by the different shRNAs, the analyses of CCL2 secretion were continued only with those shRNAs that indeed gave rise to the desired extensive and marked inhibition of HS (by shRNAs to EXT2; Figure 4*A*1) or of CS (by shRNA to CHSY1; Figure 4*A*2) expression. Taking this approach, we could show that the secretion of endogenous CCL2 was partly reduced in the absence of HS and CS, by an average of 37.6 ± 6.2% and 36.1 ± 3.8%, respectively, in the different experiments (Figure 4, *B*1 and *B*2).

These findings indicate that each of the two predominant GAGs expressed in MDA-MB-231 cells partly affects the secretion of CCL2 WT, standing in line with the partial involvement of GAGs in CCL2 secretion that was revealed for GFP-CCL2 WT in CHO cells. Here, it is important to indicate that in the course of these studies we found out that complex co-regulatory pathways exist

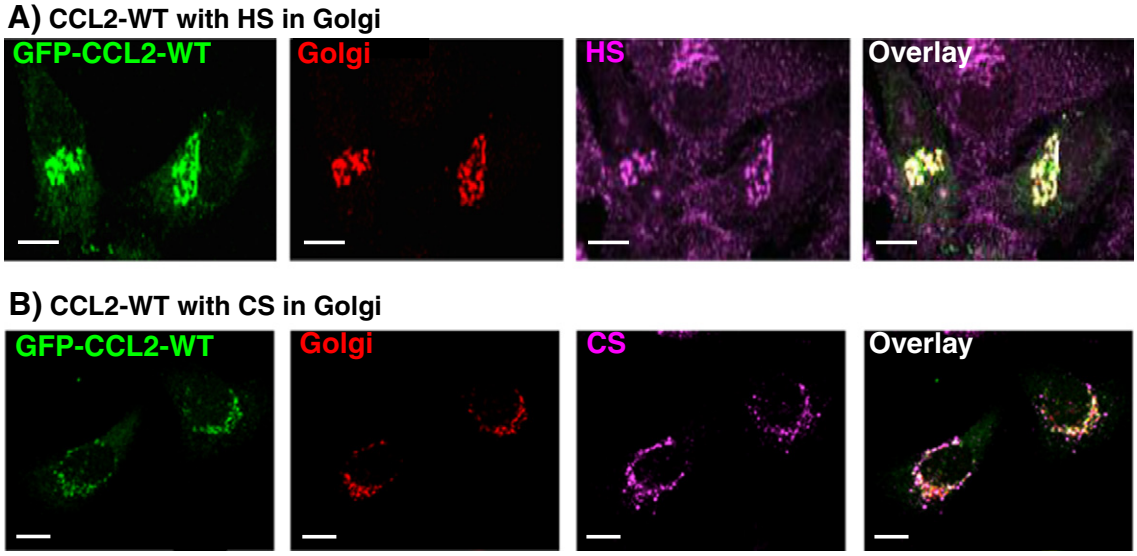

Figure 2. CCL2 WT is localized with HS and CS in the Golgi. MDA-CCL2-low cells were transfected to express GFP-CCL2 WT. After 48 hours, the intracellular localization of the chemokine was determined by confocal analyses of the GFP signal. (A) Co-localization of GFP-CCL2 WT with HS in the Golgi. The expression patterns of HS and of the Golgi marker α-mannosidase IB were determined by antibodies. (B) Co-localization of GFP-CCL2 WT with CS in the Golgi. The expression patterns of CS and of the Golgi marker α-mannosidase IB were determined by antibodies. In both parts of the figure, negative controls included staining by non-relevant isotype-matched antibodies (data not shown). The results are representatives of many pictures that were taken in $n > 3$ independent experiments. Bar, 10 μm.

between HS and CS (data not shown), due to which we decided not to run experiments in which both HS and CS were downregulated simultaneously by shRNAs to EXT2+CHSY1.

The Secretion of CCL2 WT Depends on Its GAG-Binding Domains and on Its 40s Loop

The results described so far indicate that GAGs partly mediate the secretion of CCL2. The binding of CCL2 to GAGs has been studied extensively in the past. In the presence of heparin oligosaccharides, CCL2 tetramers were formed, where a continuous ring of basic residues encircled the tetramer and created a positively charged surface that could bind GAGs. The integration of several reports indicated that R18, K19, R24, and K49 constituted the primary GAG-binding domains of CCL2 and suggested that K58 and H66 also participated in GAG binding although to a lesser extent [51,52].

To follow on this information, we designed CCL2 variants mutated in GAG-binding aa, including the R18+K19 pair that has been extensively studied for its roles in GAG binding and R24, K49, K58 or H66 (the mutants eventually used in the study are shown in Table 1). In parallel, we designed mutants that carried mutations in different combinations of two to four of these amino acids. For further analysis, we have used only those mutants whose bioinformatics Three-Dimensional (3D) structure modeling (Figure W3) and published nuclear magnetic resonance (NMR) analyses [51,66] have revealed structural integrity. These mutants included R18A+K19A, R24A and H66A, whose aa sequences are shown in Table 1.

As mentioned above, we have also addressed the role of the 40s loop of CCL2 in regulating the secretion of the chemokine. Here, we focused on the ^{45}TIVA^{48} domain in CCL2 that is equivalent to the ^{43}TRKN^{46} motif that regulated CCL5 secretion by breast tumor cells and other cell types as well [44]. Correct folding of the ^{45}TIVA^{48} mutant of CCL2 was predicted by modeling (Figure W3), and thus, a TIVA mutant (^{45}AAAA^{48}) was generated, to be named TIVA−− (Table 1). To analyze the cooperativity between GAG-binding domains and the 40s loop of CCL2, we also generated an R18A+K19A +TIVA−− mutant, which based on bioinformatics modeling carried an intact 3D structure (Figure W3 and Table 1).

Overall, the study included five CCL2 mutants: R18A+K19A, R24A, H66A, TIVA−−, and R18A+K19A+TIVA−−. All mutants were tagged by GFP in their carboxyl terminus as was previously done for the WT chemokine, GFP-CCL2 WT (Table 1). Following transfection to MDA-CCL2-low cells, the molecular weights (MWs) of the WT and mutated forms of CCL2 were determined by WB analyses following immunoprecipitation by GFP-directed antibodies. Figure W4 demonstrates the results obtained by reacting the membrane with polyclonal antibodies against CCL2; in general, similar results were obtained by reacting the membrane with monoclonal antibodies against GFP (data not shown). The WB results indicated that 1) high CCL2 expression was detected only after transfection of MDA-CCL2-low cells by GFP-CCL2 WT, whereas cells transfected by the control empty GFP vector did not show the expression of the chemokine; 2) GFP-CCL2 WT migrated in the expected MW of ~38 to 40 kDa (27 kDa of GFP + ~15 kDa of glycosylated CCL2), in two bands that probably represent the different glycosylation forms of CCL2 previously reported by others [67–69]; (3) all five GFP-CCL2 mutants migrated in the gel in the same two forms found for GFP-CCL2 WT, thus assuring their correct MWs and structures. These WB analyses, together with the bioinformatics and published NMR studies mentioned above, suggested that the CCL2 mutants could provide a solid platform for studying the roles of CCL2 domains in regulating its secretion.

After assuring the expression of GFP-CCL2 WT and the five GFP-CCL2 mutants in MDA-CCL2-low cells, the following experimental

measures were taken: 1) On the basis of GFP expression, we validated that the expression levels of the mutated chemokines were similar to those of the WT chemokine in each experiment (representative experiments are shown in Figure W5); 2) CCL2 secretion was determined by ELISAs by the same antibodies that were used in the WB analyses (WB shown in Figure W4); 3) CCL2 localization in the Golgi and in the ER was determined qualitatively and quantitatively by confocal analyses.

Taking the above approach, we began this part of the study by analyzing the R18A+K19A mutant. The secretion of this mutant by the tumor cells was inhibited by an average of 51.1 ± 13.7%, obtained in the different experiments comparing it to the WT chemokine (Figure 5*A* and Table 2). As shown previously (Figures 1*A* and 2), the GFP-CCL2 WT was highly localized in the Golgi, with only sparse expression in the ER. In comparison to the WT chemokine, the localization of GFP-CCL2-R18A+K19A was reduced by 59% in the Golgi and increased by 1.62-fold in the ER (Figure 5, *B* and *C*, and Table 2).

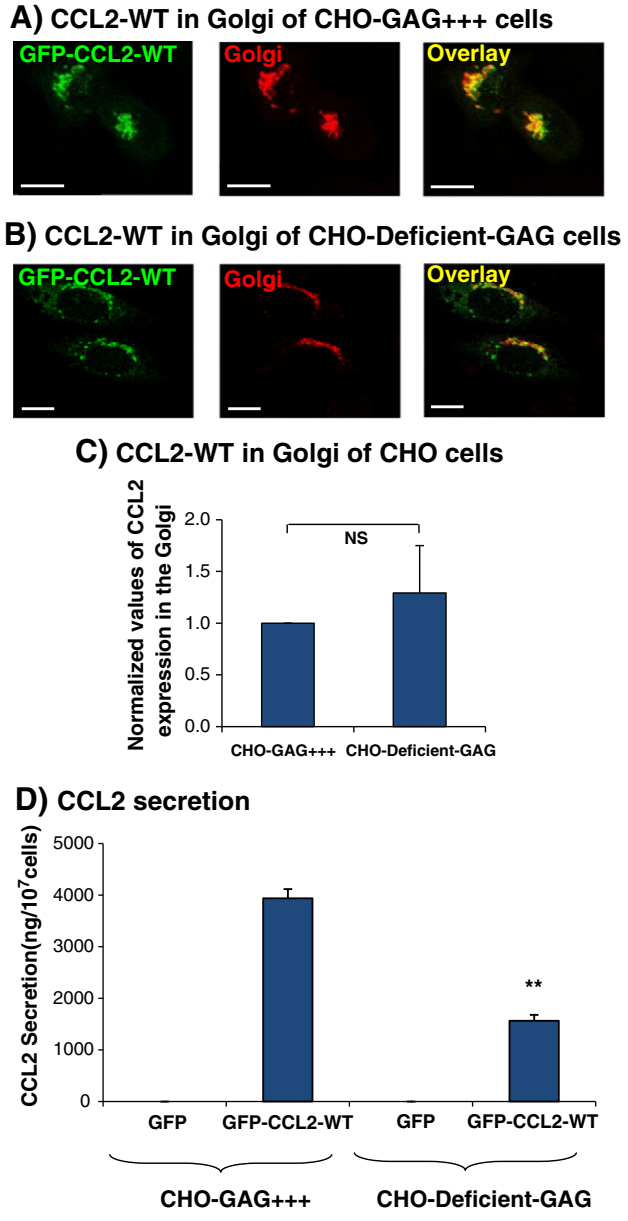

The analyses of the GFP-CCL2-R24A mutant have shown more prominent inhibition in secretion, reaching an average of 85.6 ± 2.3% reduction compared to the GFP-CCL2 WT (Figure 6*A*), indicating that R24 is a key determinant of CCL2 secretion. In comparison to the WT chemokine, the GFP-CCL2-R24A variant has shown 55% inhibition in Golgi localization and 1.67-fold elevation in ER localization (Figure 6, *B* and *C*, and Table 2). In contrast, the GFP-CCL2-H66A mutant has been distributed in the cells in a manner totally similar to that of GFP-CCL2 WT; nonetheless, the mutation in H66 has led to 46.1 ± 15.8% inhibition in its secretion (Figure 7 and Table 2).

To follow the above results with the GAG-binding domain mutants, we have determined these same characteristics for the GFP-CCL2-TIVA-- mutant of the 40s loop. Giving rise to substantial inhibition of 70.2 ± 4.3% in secretion by the tumor cells in the different experiments, the Golgi localization of this mutant was considerably reduced (by 63%) and the mutant had increased presence of 1.43-fold in the ER compared to the GFP-CCL2 WT chemokine (Figure 8 and Table 2). The experiments with the combined GFP-CCL2-R18A+K19A+TIVA-- mutant showed almost complete inhibition of secretion, at the level of 93.3 ± 9.3% in the different experiments. In parallel, the localization of this mutated CCL2 in the Golgi was reduced by 60% and its ER localization was elevated by 1.73-fold (Figure 9 and Table 2).

To conclude, the overall results obtained in this part of the study (summarized in Table 2) have identified two CCL2 domains that had particular importance in regulating the secretion of the chemokine. These were the R24 aa and the combination of R18+K19+^{45}TIVA^{48} sequences. The mutation of these two domains gave rise to inhibition of ~90% in CCL2 secretion. In parallel, the R18+K19 motif alone, the 40s loop on its own (^{45}TIVA^{48}), and the H66 aa had only partial roles in regulating the secretion of CCL2. Except for H66 that had normal intracellular localization in Golgi and ER, all other CCL2 mutations (R24A, R18A+K19A, TIVA--, and R18A+K19A+TIVA--) had

Figure 3. Intracellular GAGs are partly required for CCL2 secretion and for the transport of CCL2 WT from the Golgi toward secretion. CHO-GAG+++ cells and CHO-deficient GAG cells were transfected to express GFP-CCL2 WT. Additional characteristics of the two CHO cell types are shown in Figure W2. (A and B) Localization of GFP-CCL2 WT in the Golgi of CHO-GAG+++ and of CHO-deficient GAG cells, determined by confocal analyses of the GFP signal. In parallel to expression of GFP-CCL2 WT, the expression of the Golgi marker α-mannosidase IB was determined by antibodies. (A) The localization of GFP-CCL2 WT in the Golgi of CHO-GAG+++ cells. (B) The localization of GFP-CCL2 WT in the Golgi of CHO-deficient GAG cells. In A and B, the negative controls included staining by non-relevant isotype-matched antibodies (data not shown). The results are representatives of many pictures that were taken in $n > 3$ independent experiments. Bar, 10 μm. (C) Quantitative analyses of the co-localization obtained between GFP-CCL2 WT and the Golgi marker α-mannosidase IB in CHO-GAG+++ and in CHO-deficient GAG cells, performed by the Slidebook program. In C, the results are based on analyses of many pictures that were taken in $n > 3$ independent experiments and are presented as mean ± SD, where the values of CHO-GAG+++ cells were given the value of 1. NS, not significant. (D) The secretion of GFP-CCL2 WT by CHO-GAG+++ cells and CHO-deficient GAG cells. The levels of CCL2 in cell supernatants were determined by sandwich ELISAs, at the linear range of absorbance. $^{**}P < .01$ comparing between CCL2 secretion levels in CHO-GAG+++ cells *versus* CHO-deficient GAG cells, with inhibition levels of 59.4 ± 16.2% in the different experiments. In D, the results are representatives of $n > 3$ independent experiments.

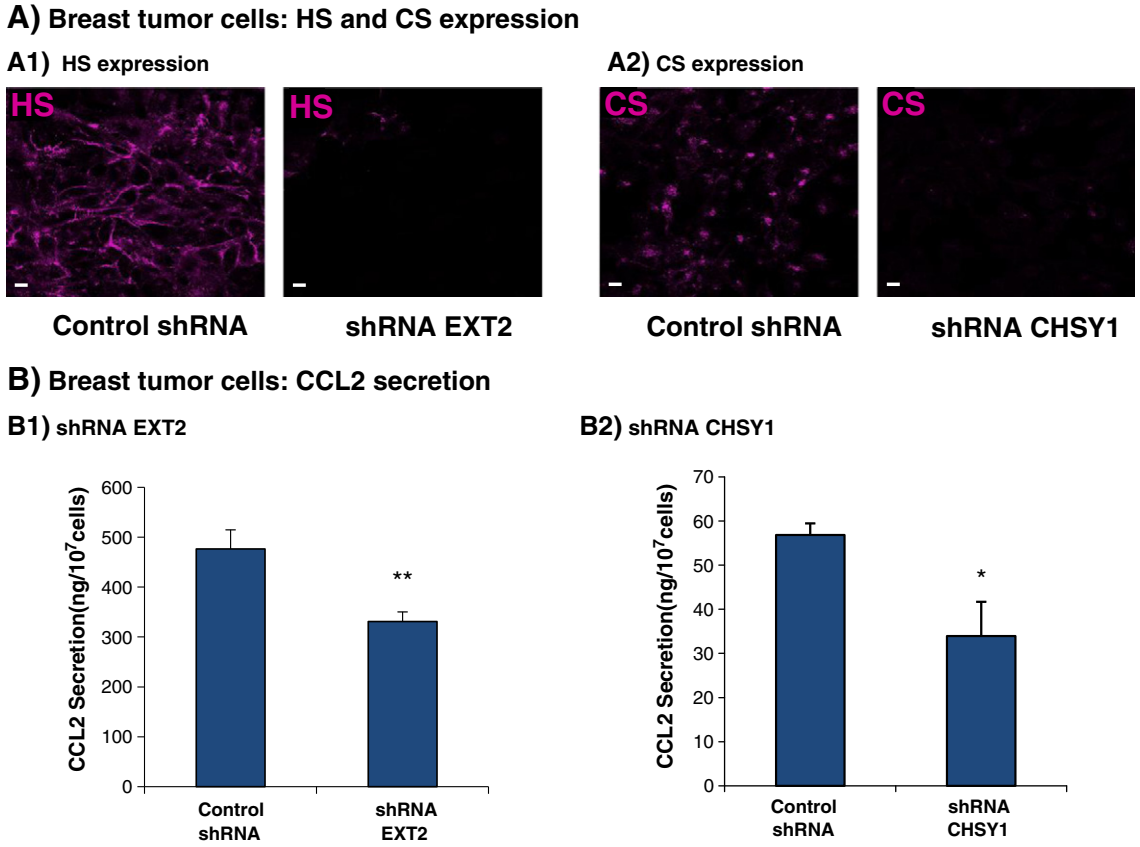

Figure 4. HS and CS partly mediate the secretion of CCL2 by breast tumor cells. MDA-CCL2-high cells were infected by shRNAs directed against the enzymes that synthesize HS or CS or by control non-relevant shRNAs. After 48 hours, the expression of HS or CS was determined, and in parallel, the secretion of endogenous CCL2 was evaluated. (A) Down-regulation of HS expression (A1) or CS expression (A2) after infection by shRNA for EXT2 (A1) or for CHSY1 (A2). The shRNAs were selected out of several shRNAs that were tested for their ability to downregulate HS or CS expression. HS or CS expression was determined by antibodies using confocal analyses. Negative controls included cells transfected by non-relevant shRNAs and staining by non-relevant isotype-matched antibodies (data not shown). In A, the results are representatives of many pictures that were taken in $n > 3$ independent experiments. Bar, 10 μm. (B) The levels of CCL2 in cell supernatants were determined by sandwich ELISA in the linear range of absorbance, in cells expressing shRNAs for EXT2 (B1) or shRNA for CHSY1 (B2). $^*P < .05$ and $^{**}P < .01$ comparing cells transfected with control shRNA and shRNAs for EXT2 or CHSY1. The inhibition levels in cells expressing shRNA downregulating EXT2 were 37.6 ± 6.2%, and for shRNA downregulating CHSY1, they were 36.1 ± 3.8%. In B, the results are representatives of $n > 3$ independent experiments.

lower propensity for Golgi localization than the WT chemokine. The implications of these findings will be addressed further below, in the Discussion section.

The Regulation of CCL2 Secretion by Its GAG-Binding Domains and 40s Loop in Other Cells

The above findings have identified specific CCL2 domains that control the secretion of CCL2 in breast tumor cells. To follow these results, we asked how general is the ability of the different CCL2 domains to regulate CCL2 secretion. Specifically, we asked if the R18+K19, R24, H66, ^{45}TIVA^{48} and R18+K19+^{45}TIVA^{48} domains regulate CCL2 secretion not only in breast tumor cells but also in other cell types. To address this question, we expressed all five mutants in native cells that were not modified in GAG expression, namely, CHO-GAG+++ and HEK 293 cells (validation of transfection yields are shown in Figures W6 and W7, respectively).

The analyses of Figure 10 indicate that the different CCL2 chemokine motifs regulated CCL2 secretion in CHO-GAG+++ cells in a pattern similar to the one revealed in breast tumor cells (Figure 10*A vs* Figures 5–9, respectively; Table 2 *vs* Table 3). In HEK 293 cells, the CCL2 variants GFP-CCL2-R24A, GFP-CCL2-TIVA––, and GFP-CCL2-R18A+K19A+TIVA–– demonstrated inhibitory characteristics similar to those in breast tumor cells and in CHO-GAG+++ cells (Figure 10*B vs* Figures 6, 8, and 9; Table 2 *vs* Table 3). In contrast, the mutations in R18+K19 and H66 were hardly inhibitory in HEK 293 cells, as indicated by the fact that the secretion of GFP-CCL2-R18A+K19A and of GFP-CCL2-H66A were minimally reduced compared to GFP-CCL2 WT (Figure 10*B vs* Figures 5 and 7; Table 2 *vs* Table 3). Thus, the intracellular components interacting with R24, ^{45}TIVA^{48} and R18+K19+^{45}TIVA^{48} were generally shared by the different cell types, while those associating with H66 and R18+K19 alone were more cell-specific (effective only in breast tumor cells and CHO-GAG+++ cells).

Discussion

CCL2 is an inflammatory chemokine that exerts prominent pro-tumoral effects in breast cancer and in numerous other malignancies. Many lines of evidence indicate that following its release by breast tumor cells, CCL2

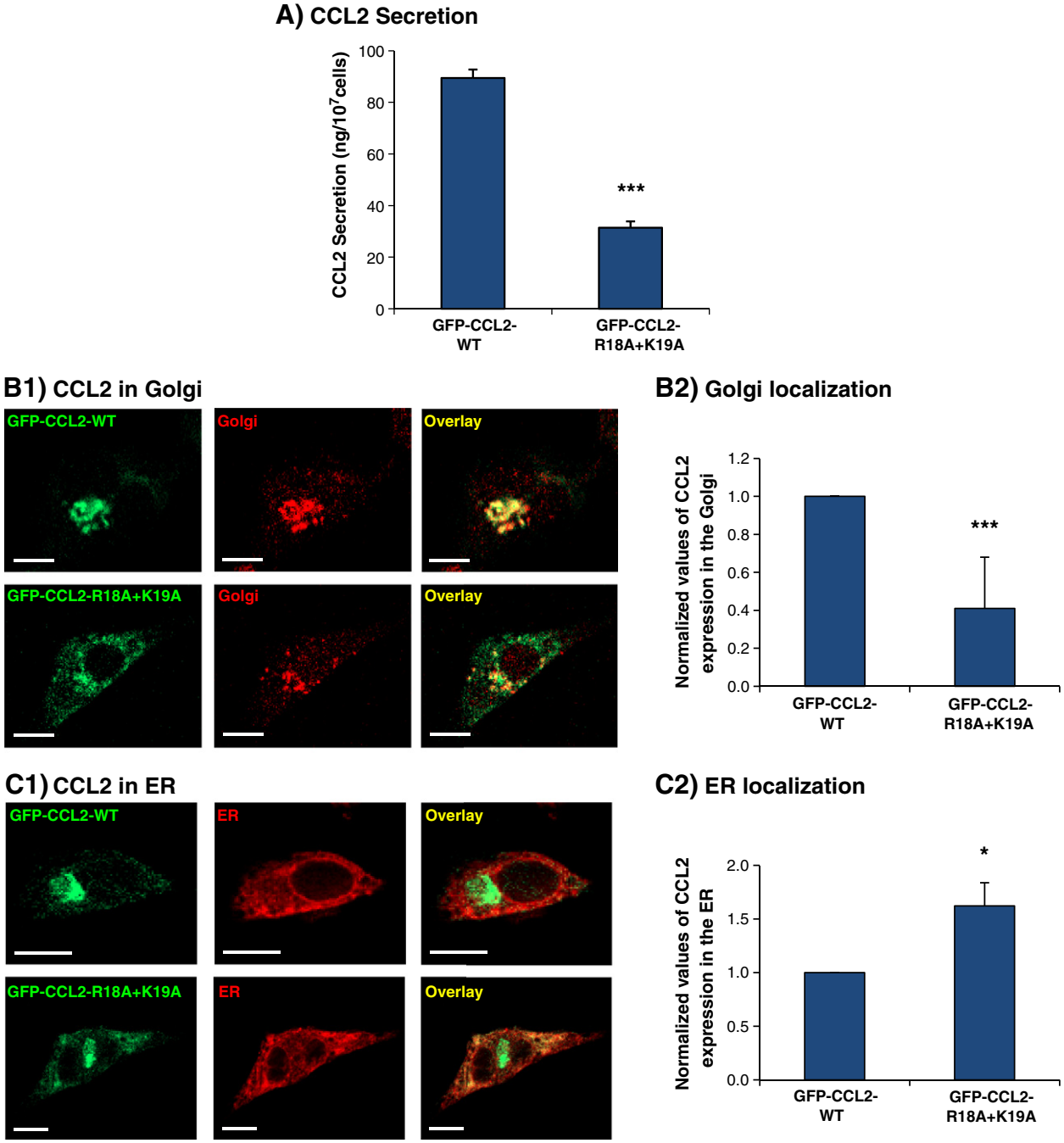

Figure 5. The secretion of GFP-CCL2-R18A+K19A by breast tumor cells is partly inhibited, and the mutated chemokine shows reduced propensity for Golgi localization. MDA-CCL2-low cells were transfected to express GFP-CCL2 WT or GFP-CCL2-R18A+K19A. Similar expression levels of GFP-CCL2-R18A+K19A, compared to GFP-CCL2 WT, were validated by FACS analyses (Figure W5*A*). (A) The levels of CCL2 in cell supernatants were determined 48 hours following transfection by sandwich ELISAs, at the linear range of absorbance. In A, the results are representatives of $n > 3$ independent experiments. (B) The expression of GFP-CCL2-R18A+K19A *versus* GFP-CCL2 WT in the Golgi was determined on the basis of the GFP signal, combined with antibodies to the Golgi marker α-mannosidase IB, using confocal analyses. Negative controls included staining by non-relevant isotype-matched antibodies (data not shown). Determination of localization was performed qualitatively (B1) and quantitatively by the Slidebook program (B2). Bar, 10 μm. (C) The expression of GFP-CCL2-R18A+K19A *versus* GFP-CCL2 WT in the ER was determined on the basis of the GFP signal combined with antibodies to the ER marker calnexin, using confocal analyses. Negative controls included staining by non-relevant isotype-matched antibodies (data not shown). Determination of localization was performed qualitatively (C1) and quantitatively by the ImageJ program (C2). Bar, 10 μm. In B1 and C1, the results are representatives of many pictures that were taken in $n > 3$ independent experiments. In B2 and C2, the results are mean ± SD values obtained from many pictures that were analyzed, where the results of GFP-CCL2 WT–expressing cells were given the value of 1. Throughout the figure, $^*P < .05$ and $^{***}P < .001$ comparing GFP-CCL2 WT and GFP-CCL2-R18A+K19A. Table 2 provides a summary of all the results presented in the figure.

Table 2. Characteristics of Secretion, Golgi Localization and ER Localization of GFP-CCL2 WT and GFP-CCL2 Mutants Following Expression in MDA-CCL2-Low Cells.

CCL2 Mutant	% Inhibition of secretion ± SD *versus* GFP-CCL2 WT	Fold Golgi localization *versus* GFP-CCL2 WT (% Inhibition)	Fold ER localization *versus* GFP-CCL2 WT
GFP-CCL2-R18A+K19A	51.1% ± 13.7	0.41 (59%)	1.62
GFP-CCL2-R24A	85.6% ± 2.3	0.45 (55%)	1.67
GFP-CCL2-H66A	46.1% ± 15.8	1.01 (0%)	1.02
GFP-CCL2-TIVA--	70.2% ± 4.3	0.37 (63%)	1.43
GFP-CCL2-R18A+K19A+TIVA--	93.3% ± 9.3	0.4 (60%)	1.73

The table summarizes the results of Figures 5 to 9 on inhibition levels of CCL2 secretion by breast tumor cells, presented as mean ± SD of the results obtained for each mutant in at least $n = 3$ independent experiments. In addition, the table summarizes the data presented in Figures 5 to 9 on Golgi and ER localization of each mutant compared to the WT chemokine. The results on Golgi and ER localization are based on analyses of many pictures that were taken in $n > 3$ independent experiments, where the values of GFP-CCL2 WT were given the value of 1.

promotes pro-malignancy activities at the tumor microenvironment and in the cancer cells and contributes to increased tumor growth and progression.

In this study, we have identified key regulatory events that control the process of CCL2 secretion by breast tumor cells (Scheme W1). We have shown that GAGs, specifically HS and CS, partly mediate the shuttling of CCL2 toward secretion and have pinpointed CCL2 domains that control its secretion. We have also identified the stages along the ER-to-Golgi trafficking process through which each domain may regulate the CCL2 secretion process, as will be described below. Our findings suggest that specific CCL2 domains regulate the secretion process by interacting with intracellular GAGs and/or with other intrinsic components and indicate that CCL2 secretion is controlled at many different stages along the secretory path.

Below, we describe the novel findings revealed in this study, their contribution to the way we conceive the mechanisms regulating chemokine secretion, and their implications to potential points of intervention in cancer in general (see also Conclusions section).

1. Intracellular GAGs in general, and HS and CS in particular, constitute an important mechanism that mediates the secretion of CCL2.

This conclusion is supported by many of the experimental approaches taken in the study, including the comparisons of CCL2 WT secretion by CHO-GAG+++ and CHO-deficient GAG cells, the experiments in which HS and CS were downregulated by shRNAs (to EXT2 and CHSY1), and the secretion phenotypes of CCL2 variants mutated in GAG-binding domains. Further below, we discuss the overall implications of GAG roles in secretion, particularly of chemokines, but we also wish to point out that based on our results GAGs are only partly involved in the process of CCL2 secretion. The question is therefore which other cellular components regulate CCL2 release by the cells. On the basis of the fact that there is an overlap between the GAG-binding motifs and CCR2b-binding domains of CCL2 (e.g., amino acids R24 and K49, binding CCR2 as monomers [51,66]), we inquired in the study also the possibility that the main CCL2 receptor, CCR2b, mediates the secretion of CCL2 by the cells. To analyze this possibility, we determined the secretion levels of GFP-CCL2 WT by native HEK 293 cells that do not express CCR2b endogenously, compared to CCR2b-overexpressing HEK 293 cells. We found that CCR2b overexpression did not lead to up-regulation of CCL2 WT secretion but rather the experiments suggested that the receptor may trap the secreted chemokine and lead to its internalization (data not shown). These experiments pointed to more complex mechanisms than initially expected, and they will have to be followed by designated studies that would address the roles of CCR2b in regulating the extracellular levels of CCL2 and the roles of different CCL2 domains in its internalization by CCR2b.

2. In the process of CCL2 secretion, GAGs affect the step in which the chemokine is directed from the Golgi toward secretion.

This conclusion is made based on the fact that CCL2 has normally reached the Golgi apparatus in CHO-deficient GAG cells, but nevertheless, its secretion was inhibited by 59.4 ± 16.2% in these cells. This finding agrees well with the fact that the key steps of GAG synthesis—including HS and CS—take place in the Golgi [63–65]. The implications of this finding are that CCL2 reaches the Golgi in a GAG-independent process and moves from the Golgi toward secretion in a process that is GAG-dependent.

3. The process of CCL2 secretion is regulated by multiple CCL2 domains, including typical GAG-binding domains and the 40s loop.

Our findings indicate that CCL2 secretion by breast tumor cells is coordinated by several chemokine domains. The Golgi and ER localization phenotypes of the different mutants have also suggested that each domain contributes its share to specific steps of the ER-to-Golgi-secretion route taken by the chemokine (Scheme W1).

Below, we propose our interpretations of the roles played by each CCL2 domain in these processes. As a word of caution, we would like to mention that elevated ER localization of some of the mutants could have been not only due to the roles of CCL2 domains in ER-to-Golgi trafficking but also because of "saturation" of the secretory pathway or some folding issues. Yet, we would like to note that 1) all mutants were compared to the WT form of the chemokine that provides the background levels of ER localization, under conditions in which the chemokine occupies the secretory pathway to its outmost levels (because it is the WT form that is highly secreted); 2) our WB analyses indicated that all CCL2 mutants had the correct MW and the bioinformatics studies suggested that all mutants had intact structure. Correct folding of the mutants was greatly supported by the published NMR analyses, demonstrating correct 3D structure of all the GAG-binding mutants used in our study.

Taking all the above considerations into account, we wish to address first the regulation of CCL2 secretion and intracellular trafficking by the GAG-binding domains of CCL2. In this study, we have addressed the GAG-binding domains R18+K19, R24 and H66. Our analyses suggest that each of these domains participates in definite, and not necessarily overlapping, stages of the process: 1) H66—The secretion of GFP-CCL2-H66A was inhibited by 46.1% in breast tumor cells. Since the chemokine has reached normally the Golgi in these cells, its reduced secretion must have been the result of it lower ability to proceed from the Golgi toward secretion. As discussed above, we have shown that the GAG-dependent process of CCL2 secretion is the post-Golgi stage. Thus, we suggest that H66 mediates the interaction of CCL2 WT with GAGs that shuttle the chemokine from the Golgi toward secretion; 2) R24—Mutation in R24 (GFP-CCL2-R24A) has led to 85.6% inhibition of CCL2 secretion, accompanied by only 55% reduction in its ability to reach the Golgi in breast tumor cells. Thus, the R24A-mutated chemokine could partly proceed to the Golgi, but those molecules that reached the Golgi did not fully traffic toward secretion. This means that the R24 aa regulates two steps of the secretion process: the GAG-dependent phase of Golgi to secretion and the GAG-independent stage of ER-to-Golgi trafficking. The previous identification of R24 as a major GAG-binding domain of CCL2 suggests that R24 mediates

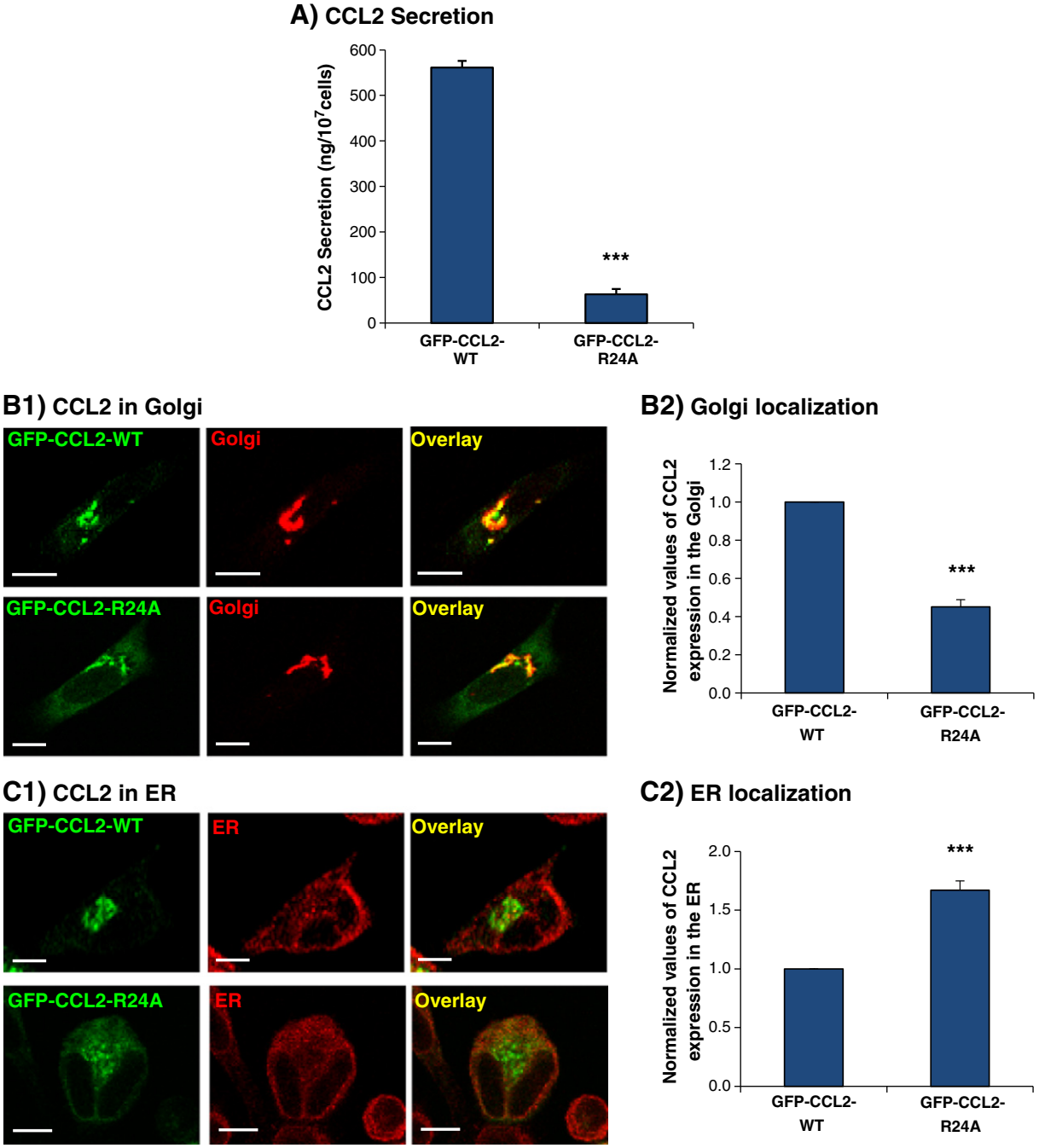

Figure 6. The secretion of GFP-CCL2-R24A by breast tumor cells is almost completely inhibited, and the mutated chemokine shows reduced propensity for Golgi localization. MDA-CCL2-low cells were transfected to express GFP-CCL2 WT or GFP-CCL2-R24A. Similar expression levels of GFP-CCL2-R24A compared to GFP-CCL2 WT were validated by FACS analyses (Figure W5*B*). All additional details (including number of repeats and modes of data presentation) are similar to those of Figure 5, albeit with the GFP-CCL2-R24A mutant. Throughout the figure, ***$P < .001$ comparing GFP-CCL2 WT and GFP-CCL2-R24A. Bar, 10 μm. Table 2 provides a summary of all the results presented in the figure.

the binding of CCL2 to GAGs in the post-Golgi stage, but that it can also regulate the step of ER exit, possibly by binding to non-GAG components that control the trafficking of the chemokine from the ER to the Golgi; 3) R18+K19—The double mutant GFP-CCL2-R18A+K19A has shown 51.1% inhibition in secretion and similar levels of reduction in Golgi localization in breast tumor cells. These findings indicate that the inhibition of the R18A+K19A mutant takes place at the ER-to-Golgi stage that is the non–GAG-dependent step of CCL2 shuttling toward secretion. Therefore, despite its being a GAG-binding domain, the R18+K19 region probably regulates the non–GAG-dependent stage of ER-to-Golgi mobilization.

To follow on the above, the analyses of the 40s loop have indicated that the ^{45}TIVA^{48} sequence, alone or in combination with the R18+K19 motif, plays distinct roles in regulating CCL2 secretion and intracellular trafficking: 1) The ^{45}TIVA^{48} sequence—The secretion of the GFP-CCL2-TIVA-- mutant was inhibited by

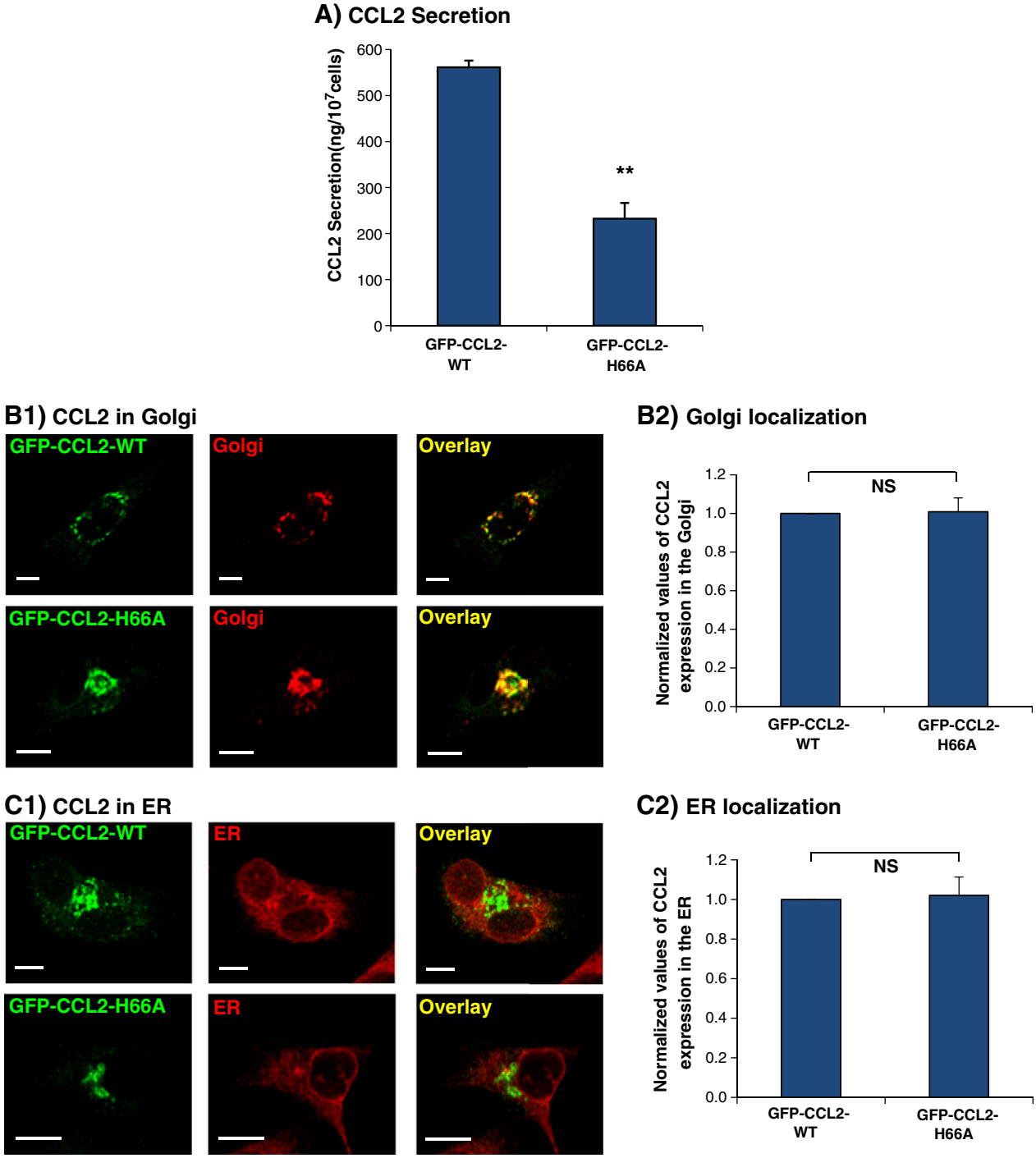

Figure 7. The secretion of GFP-CCL2-H66A by breast tumor cells is partly inhibited, and the mutated chemokine shows normal Golgi and ER localization. MDA-CCL2-low cells were transfected to express GFP-CCL2 WT or GFP-CCL2-H66A. Similar expression levels of GFP-CCL2-H66A compared to GFP-CCL2 WT were validated by FACS analyses (Figure W5*C*). All additional details (including number of repeats and modes of data presentation) are similar to those of Figure 5, albeit with the GFP-CCL2-H66A mutant. Throughout the figure, $^{**}P < .01$ comparing GFP-CCL2 WT and GFP-CCL2-H66A. NS, not significant. Bar, 10 μm. Table 2 provides a summary of all the results presented in the figure.

70.2% and the mutated chemokine showed 63% reduction in reaching the Golgi in breast tumor cells. Thus, the ^{45}TIVA^{48} domain of CCL2 was required mostly for the ER-to-Golgi step that is the GAG-independent stage of the process. Indeed, the ^{45}TIVA^{48} motif is not expected to regulate the process by interacting with GAGs because it is not one of the GAG-binding domains of CCL2. Rather, the ^{45}TIVA^{48} stretch probably mediates the interactions of CCL2 with as yet unidentified other intracellular components that regulate the exit of the chemokine from the ER. Here, it is interesting to note that the 40s loop was found in the past to control the positioning of other chemokines—CCL5, CXCL8 and CXCL4—in secretory organelles. Only in the case of CCL5 the 40s loop

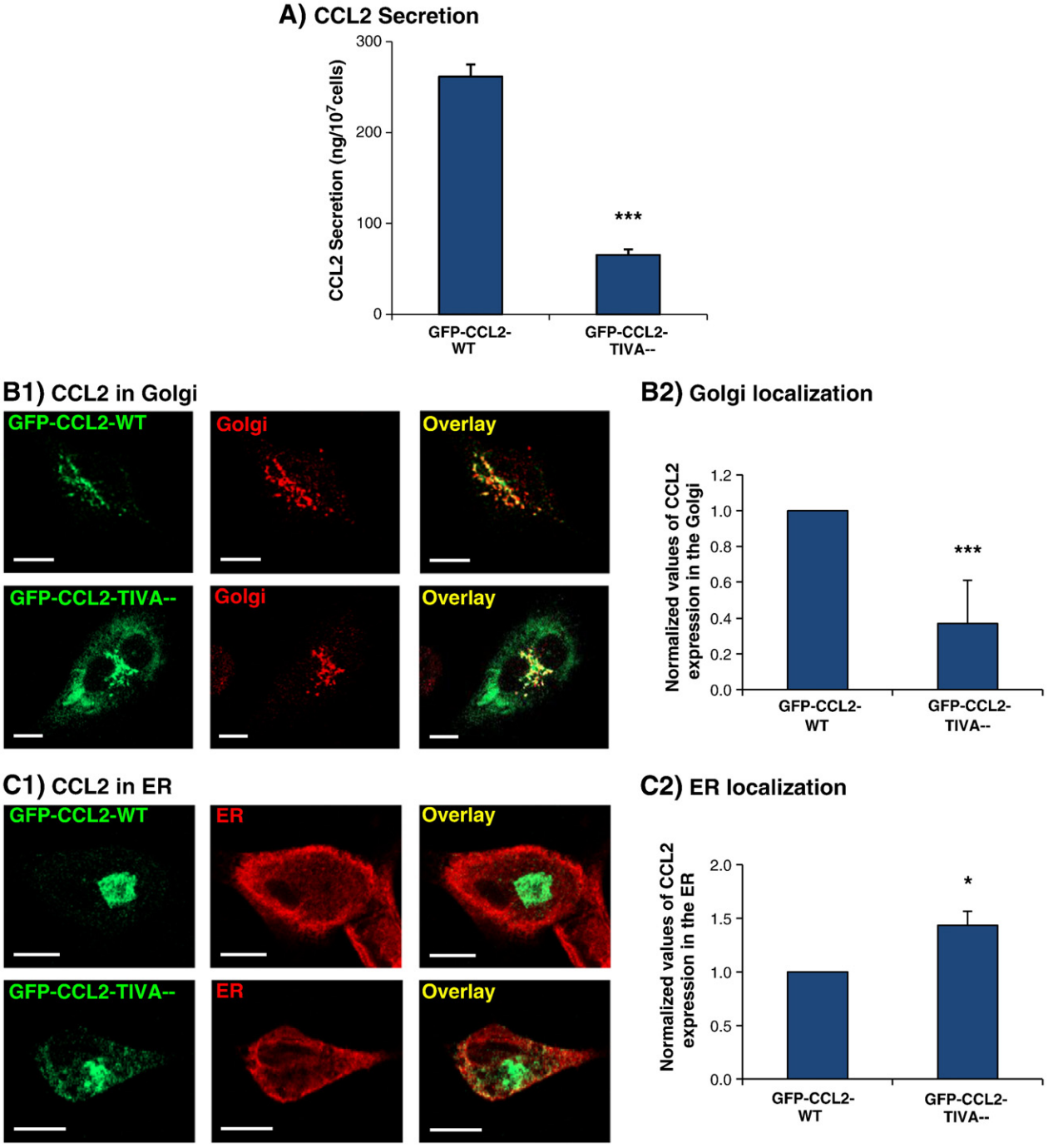

Figure 8. The secretion of GFP-CCL2-TIVA−− by breast tumor cells is partly inhibited, and the mutated chemokine shows reduced propensity for Golgi localization. MDA-CCL2-low cells were transfected to express GFP-CCL2 WT or GFP-CCL2-TIVA−−. Similar expression levels of GFP-CCL2-TIVA−− compared to GFP-CCL2 WT were validated by FACS analyses (Figure W5*D*). All additional details (including number of repeats and modes of data presentation) are similar to those of Figure 5, albeit with the GFP-CCL2-TIVA−− mutant. Throughout the figure, $*P < .05$ and $***P < .001$ comparing GFP-CCL2 WT and GFP-CCL2-TIVA−−. Bar, 10 μm. Table 2 provides a summary of all the results presented in the figure.

consisted of a positively charged, GAG-binding sequence (^{43}TRKN^{46}); in contrast, most of the aa of the 40s domains of CXCL8 and CXCL4—^{44}SDG^{46} in CXCL8 and ^{45}LKNG^{48} in CXCL4 [49,50]—are not charged, and indeed, these motifs are not the GAG-binding domains of these two chemokines. It is possible that the exposed nature of the 40s loop in all these three latter chemokines—CCL2, CXCL8, and CXCL4—enables their interaction with intracellular components that direct the positioning of these chemokines in secretory organelles; 2) The ^{45}TIVA^{48} sequence combined with the R18+K19 motif—The R18A+K19A +TIVA−− mutant has shown an interesting phenotype, in which its secretion was almost completely inhibited in breast tumor cells (93.3%), but its Golgi localization was reduced by 60% only. Thus, this double mutant may interact with intracellular components that

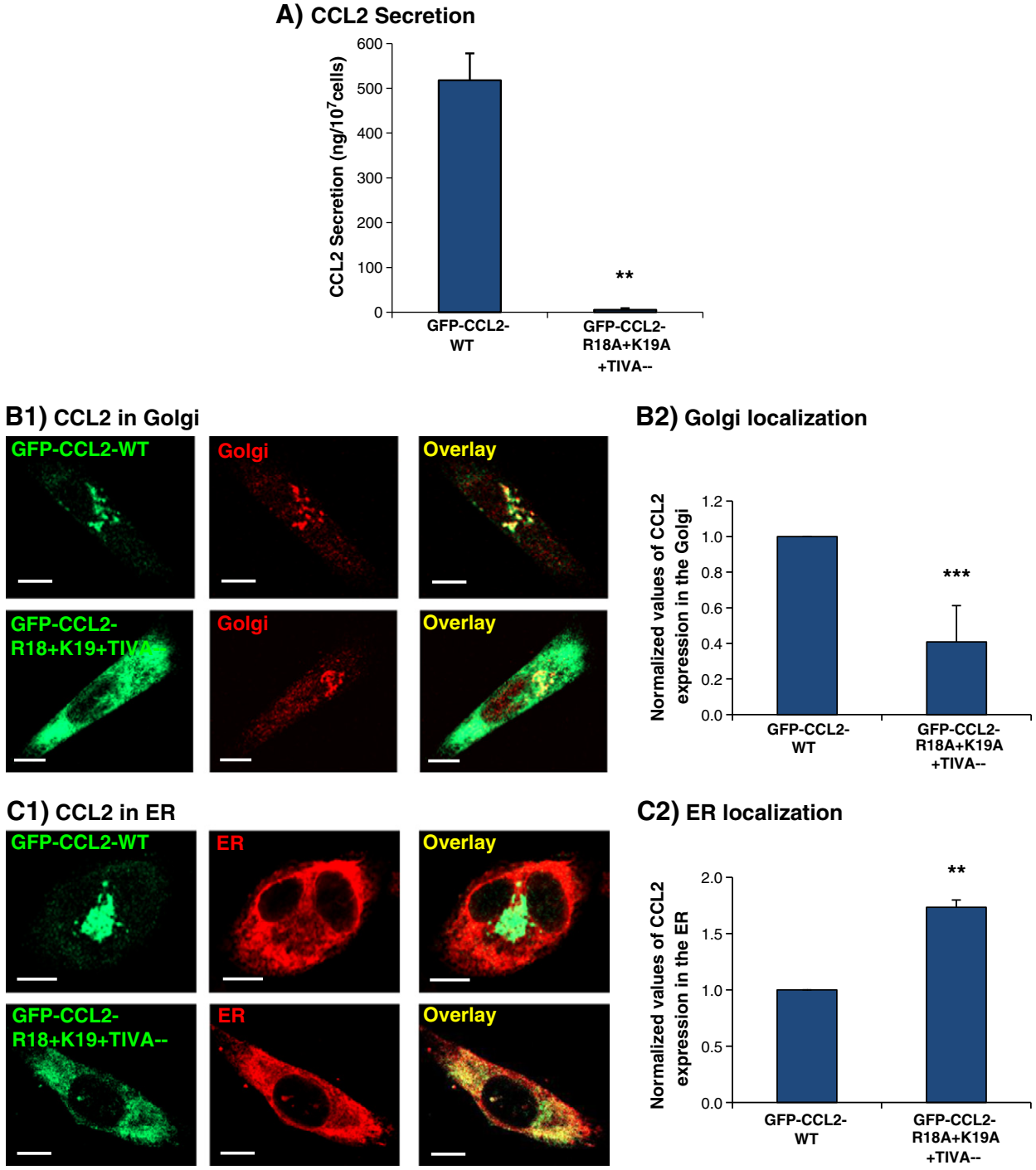

Figure 9. The secretion of GFP-CCL2-R18A+K19A+TIVA−− by breast tumor cells is completely inhibited, and the mutated chemokine shows reduced propensity for Golgi localization. MDA-CCL2-low cells were transfected to express GFP-CCL2 WT or GFP-CCL2-R18A +K19A+TIVA−−. Similar expression levels of GFP-CCL2-R18A+K19A+TIVA−− compared to GFP-CCL2 WT were validated by FACS analyses (Figure W5*E*). All additional details (including number of repeats and modes of data presentation) are similar to those of Figure 5, albeit with the GFP-CCL2-R18A+K19A+TIVA−− mutant. Throughout the figure, $^{**}P < .01$ and $^{***}P < .001$ comparing GFP-CCL2 WT and GFP-CCL2-R18A+K19A+TIVA−−. Bar, 10 μm. Table 2 provides a summary of all the results presented in the figure.

regulate the process of ER-to-Golgi trafficking and of the post-Golgi, as well. It is possible that in this double mutant, each domain has assumed the ability to regulate a separate stage of the process or alternatively that there was an overlap in which each of the two domains similarly regulated the process.

The results obtained in our study also suggest that there may be combinatorial effects to different CCL2 motifs in regulating the secretion process of the chemokine. CCL2 tetramers are those that most efficiently bind extracellular GAGs. If such tetramers are formed intracellularly, then the domains that we have identified may

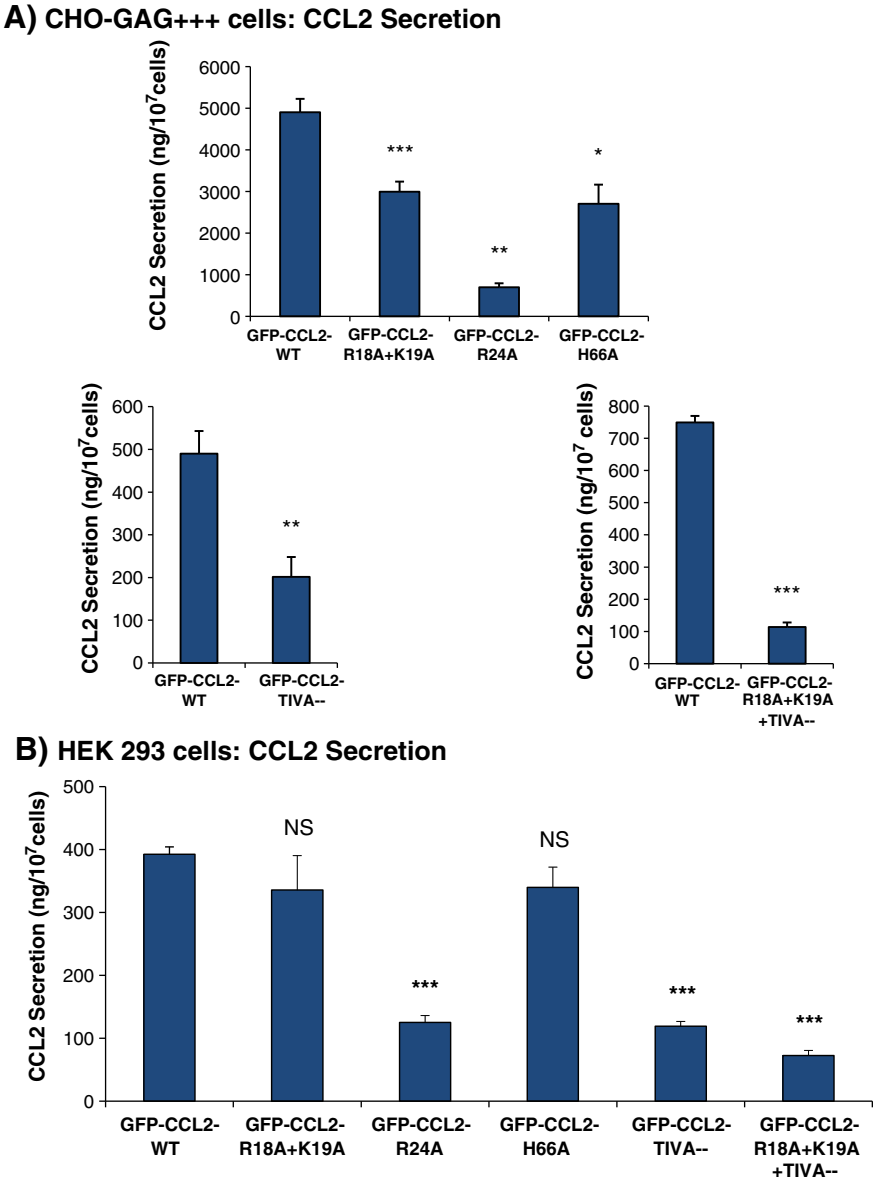

Figure 10. The general use of CCL2 GAG-binding domains and its 40s loop by different cell types. CHO-GAG+++ cells (A) and HEK 293 cells (B) were transfected to express GFP-CCL2 WT or GFP-CCL2 mutants: GFP-CCL2-R18A+K19A, GFP-CCL2-R24A, GFP-CCL2-H66A, GFP-CCL2-TIVA−−, and GFP-CCL2-R18A+K19A+TIVA−−. Similar expression levels of the WT and mutated variants of CCL2 were validated by FACS analyses (Figure W6 for CHO-GAG+++ cells and Figure W7 for HEK 293 cells). The levels of CCL2 in cell supernatants were determined 48 hours following transfection by sandwich ELISAs, at the linear range of absorbance. $*P < .05$, $**P < .01$ and $***P < .001$ for GFP-CCL2 mutants compared to GFP-CCL2 WT. NS, not significant. The results are representatives of $n \geq 3$ independent experiments. Table 3 provides a summary of all the results.

act in a combinatorial manner to regulate the different stages of the trafficking process of CCL2 toward secretion. For example, it is possible that in the tetramer there will be cooperativity between H66 that controls the GAG-dependent post-Golgi stage and R24 that controls the non–GAG-dependent ER-to-Golgi step. The results obtained above with the R18A+K19A+TIVA−− mutant strongly support such cooperativity between the different CCL2 domains. This combined mutant has acquired a phenotype that was similar (regulating the ER-to-Golgi stage) but also partly extended (regulating the Golgi-to-secretion stage) when compared to each single mutant (R18A+K19A or TIVA−−). Therefore, it is possible that when the R18+K19 motif was joined by the ^{45}TIVA^{48} domain, its GAG-binding activities have enabled it to mediate also the GAG-dependent stage of Golgi toward secretion.

Overall, we have identified CCL2 domains that regulate its secretion and intracellular trafficking and have demonstrated key, although partial, roles for intracellular GAGs in the process.

Conclusions

The findings of our study shed light on the complexity of the process that transports CCL2 toward secretion and set an important role to GAGs in this process. These observations add to our current understanding of the way GAGs affect different cellular processes. Several recent studies have suggested that intracellular GAGs have key

Table 3. The Secretion Levels of GFP-CCL2 WT and GFP-CCL2 Mutants by CHO-GAG+++ Cells and HEK 293 Cells.

CCL2 Mutant	CHO-GAG+++ Cells: % Inhibition of Secretion ± SD *versus* GFP-CCL2 WT	HEK 293 Cells: % Inhibition of Secretion ± SD *versus* GFP-CCL2 WT
GFP-CCL2-R18A+K19A	46.9 ± 32	19.7 ± 13.4
GFP-CCL2-R24A	72.3 ± 13.4	69.6 ± 12.1
GFP-CCL2-H66A	36.9 ± 13	19.4 ± 4.8
GFP-CCL2-TIVA––	59.6 ± 17.5	69.7 ± 7.8
GFP-CCL2-R18A+K19A+TIVA––	84.8 ± 3	86.6 ± 9.4

The table summarizes the results of Figure 10 on inhibition levels of CCL2 secretion by CHO-GAG+++ cells and HEK 293 cells. For each mutant, the mean ± SD values were obtained from at least $n = 3$ independent experiments, calculated compared to GFP-CCL2 WT.

roles in delivering proteins to the cell membrane or to the extracellular milieu of cells [70]. Functional interactions with HS proteoglycans were shown to be essential for the export of FGF-2, and HS was also found to be involved in insulin secretion [71,72]. Specifically for chemokines, our current research on CCL2 extends several previous studies that addressed the roles of GAGs and GAG-binding domains of chemokines in secretion: The first was our published study that has identified the GAG-binding 40s domain of CCL5 and GAGs as essential components required for its secretion [44]; the second was the study by Luster and colleagues showing that cytotoxic T cells secreted CCL5, CCL3 and CCL4 as macromolecular complexes containing sulfated proteoglycans [73]. Another related publication indicated that the core protein of serglycin is involved in the secretion of CXCL1 by endothelial cells [74]. Overall, there is a growing body of evidence suggesting key roles for GAGs in regulating secretory processes, and in the case of chemokines, this activity agrees well with the major role of GAGs in presenting chemokines to leukocytes, promoting their transendothelial migration to inflamed tissues.

On the basis of our results in this study, we propose that the secretion of CCL2 by breast tumor cells and consequently the tumor-promoting activities of this chemokine could be inhibited by modalities that would target the interactions of CCL2 with intracellular components. Here, a most intriguing candidate is R24, a single aa that has an essential role in regulating CCL2 secretion in breast tumor cells but also in other cell types, suggesting that the intracellular component/s binding this aa are shared by many cell types. Therefore, it is expected that modalities targeting CCL2 domains, particularly R24 (through measures that we have already started to design), may be effective not only in breast tumor cells but may also inhibit the secretion of this tumor-promoting chemokine by other cells of the tumor microenvironment, leukocytes and stroma cells alike.

Such a possible strategy of CCL2 inhibition can lead to reduced expression of the chemokine in breast tumors; this may apply to other malignancies as well, because CCL2 is considered as a tumor-promoting factor in many cancer diseases [5–14]. The question is whether such modalities will impact the ability of the host to mount inflammatory processes in response to infection. Our assumption is that they will not, because of the high redundancy that characterizes the chemokine superfamily, suggesting that several other chemokines could take over the missing activities of CCL2 and induce monocyte and T cell migration in times of infection. One of them is CCL5, whose mechanism of secretion depends on the ^{43}TRKN^{45} motif and not on R24 or any of the other domains required for CCL2 secretion, and thus, CCL5 is not expected to be affected by inhibitory measures directed against chemokine sequences that regulate the secretion of CCL2.

To conclude, we propose that the observations made in our study open novel avenues for CCL2 inhibition that may target its activities in cancer while not threatening the overall immune integrity of the host.

Acknowledgements

This study was supported by Federico Foundation. The authors thank Ronen Alon (Weizmann Institute, Rehovot, Israel) for his helpful insights.

Appendix A. Supplementary data

Supplementary data to this article can be found online at http://dx.doi.org/10.1016/j.neo.2014.08.004.

References

[1] Colotta F, Allavena P, Sica A, Garlanda C, and Mantovani A (2009). Cancer-related inflammation, the seventh hallmark of cancer: links to genetic instability. *Carcinogenesis* **30**, 1073–1081.
[2] Grivennikov SI, Greten FR, and Karin M (2010). Immunity, inflammation, and cancer. *Cell* **140**, 883–899.
[3] Hanahan D and Coussens LM (2012). Accessories to the crime: functions of cells recruited to the tumor microenvironment. *Cancer Cell* **21**, 309–322.
[4] Balkwill FR and Mantovani A (2012). Cancer-related inflammation: common themes and therapeutic opportunities. *Semin Cancer Biol* **22**, 33–40.
[5] Borsig L, Wolf MJ, Roblek M, Lorentzen A, and Heikenwalder M (2013). Inflammatory chemokines and metastasis—tracing the accessory. *Oncogene* **33**, 3217–3224.
[6] Conti I and Rollins BJ (2004). CCL2 (monocyte chemoattractant protein-1) and cancer. *Semin Cancer Biol* **14**, 149–154.
[7] Leibovich-Rivkin T. L-HY, Lerrer S., Weitzenfeld P., Ben-Baruch A. (2013). *The versatile world of inflammatory chemokines in cancer*. Editor (ed)^(eds). Springer: City, pp. 135–176.
[8] Eferl R (2013). CCL2 at the crossroad of cancer metastasis. *JAKSTAT* **2**, e23816.
[9] Yadav A, Saini V, and Arora S (2010). MCP-1: chemoattractant with a role beyond immunity: a review. *Clin Chim Acta* **411**, 1570–1579.
[10] Huang B, Lei Z, Zhao J, Gong W, Liu J, Chen Z, Liu Y, Li D, Yuan Y, and Zhang GM, et al (2007). CCL2/CCR2 pathway mediates recruitment of myeloid suppressor cells to cancers. *Cancer Lett* **252**, 86–92.
[11] Soria G and Ben-Baruch A (2008). The inflammatory chemokines CCL2 and CCL5 in breast cancer. *Cancer Lett* **267**, 271–285.
[12] Verma R, Bowen RL, Slater SE, Mihaimeed F, and Jones JL (2012). Pathological and epidemiological factors associated with advanced stage at diagnosis of breast cancer. *Br Med Bull* **103**, 129–145.
[13] Ben-Baruch A (2012). The Inflammatory CC Chemokines CCL2 and CCL5 in Malignancy: Leukocyte Migration and Beyond. In: Ben-Baruch A, editor. Emirate of Sharjah: Bentham Science Publishers; 2012. p. 99–114.
[14] Craig MJ and Loberg RD (2006). CCL2 (Monocyte Chemoattractant Protein-1) in cancer bone metastases. *Cancer Metastasis Rev* **25**, 611–619.
[15] Soria G, Ofri-Shahak M, Haas I, Yaal-Hahoshen N, Leider-Trejo L, Leibovich-Rivkin T, Weitzenfeld P, Meshel T, Shabtai E, and Gutman M, et al (2011). Inflammatory mediators in breast cancer: Coordinated expression of TNFα & IL-1β with CCL2 & CCL5 and effects on epithelial-to-mesenchymal transition. *BMC Cancer* **11**, 130–149.
[16] Chavey C, Bibeau F, Gourgou-Bourgade S, Burlinchon S, Boissiere F, Laune D, Roques S, and Lazennec G (2007). Oestrogen receptor negative breast cancers exhibit high cytokine content. *Breast Cancer Res* **9**, R15.
[17] Soria G, Yaal-Hahoshen N, Azenshtein E, Shina S, Leider-Trejo L, Ryvo L, Cohen-Hillel E, Shtabsky A, Ehrlich M, and Meshel T, et al (2008). Concomitant expression of the chemokines RANTES and MCP-1 in human breast cancer: a basis for tumor-promoting interactions. *Cytokine* **44**, 191–200.
[18] Goede V, Brogelli L, Ziche M, and Augustin HG (1999). Induction of inflammatory angiogenesis by monocyte chemoattractant protein-1. *Int J Cancer* **82**, 765–770.
[19] Neumark E, Sagi-Assif O, Shalmon B, Ben-Baruch A, and Witz IP (2003). Progression of mouse mammary tumors: MCP-1-TNFα cross-regulatory pathway and clonal expression of promalignancy and antimalignancy factors. *Int J Cancer* **106**, 879–886.

[20] Low-Marchelli JM, Ardi VC, Vizcarra EA, van Rooijen N, Quigley JP, and Yang J (2013). Twist1 induces CCL2 and recruits macrophages to promote angiogenesis. *Cancer Res* **73**, 662–671.

[21] Ueno T, Toi M, Saji H, Muta M, Bando H, Kuroi K, Koike M, Inadera H, and Matsushima K (2000). Significance of macrophage chemoattractant protein-1 in macrophage recruitment, angiogenesis, and survival in human breast cancer. *Clin Cancer Res* **6**, 3282–3289.

[22] Lu X and Kang Y (2009). Chemokine (C-C motif) ligand 2 engages CCR2+ stromal cells of monocytic origin to promote breast cancer metastasis to lung and bone. *J Biol Chem* **284**, 29087–29096.

[23] Qian BZ, Li J, Zhang H, Kitamura T, Zhang J, Campion LR, Kaiser EA, Snyder LA, and Pollard JW (2011). CCL2 recruits inflammatory monocytes to facilitate breast-tumour metastasis. *Nature* **475**, 222–225.

[24] Nakasone ES, Askautrud HA, Kees T, Park JH, Plaks V, Ewald AJ, Fein M, Rasch MG, Tan YX, and Qiu J, et al (2012). Imaging tumor-stroma interactions during chemotherapy reveals contributions of the microenvironment to resistance. *Cancer Cell* **21**, 488–503.

[25] Arendt LM, McCready J, Keller PJ, Baker DD, Naber SP, Seewaldt V, and Kuperwasser C (2013). Obesity promotes breast cancer by CCL2-mediated macrophage recruitment and angiogenesis. *Cancer Res* **73**, 6080–6093.

[26] Zhang Y, Yang P, Sun T, Li D, Xu X, Rui Y, Li C, Chong M, Ibrahim T, and Mercatali L, et al (2013). miR-126 and miR-126* repress recruitment of mesenchymal stem cells and inflammatory monocytes to inhibit breast cancer metastasis. *Nat Cell Biol* **15**, 284–294.

[27] Kinder M, Chislock E, Bussard KM, Shuman L, and Mastro AM (2008). Metastatic breast cancer induces an osteoblast inflammatory response. *Exp Cell Res* **314**, 173–183.

[28] Bussard KM, Okita N, Sharkey N, Neuberger T, Webb A, and Mastro AM (2010). Localization of osteoblast inflammatory cytokines MCP-1 and VEGF to the matrix of the trabecula of the femur, a target area for metastatic breast cancer cell colonization. *Clin Exp Metastasis* **27**, 331–340.

[29] Yoshimura T, Howard OM, Ito T, Kuwabara M, Matsukawa A, Chen K, Liu Y, Liu M, Oppenheim JJ, and Wang JM (2013). Monocyte chemoattractant protein-1/CCL2 produced by stromal cells promotes lung metastasis of 4T1 murine breast cancer cells. *PLoS One* **8**, e58791.

[30] Allavena P, Sica A, Solinas G, Porta C, and Mantovani A (2008). The inflammatory micro-environment in tumor progression: the role of tumor-associated macrophages. *Crit Rev Oncol Hematol* **66**, 1–9.

[31] Murdoch C, Muthana M, Coffelt SB, and Lewis CE (2008). The role of myeloid cells in the promotion of tumour angiogenesis. *Nat Rev Cancer* **8**, 618–631.

[32] Hembruff SL, Jokar I, Yang L, and Cheng N (2010). Loss of transforming growth factor-β signaling in mammary fibroblasts enhances CCL2 secretion to promote mammary tumor progression through macrophage-dependent and -independent mechanisms. *Neoplasia* **12**, 425–433.

[33] Keeley EC, Mehrad B, and Strieter RM (2008). Chemokines as mediators of neovascularization. *Arterioscler Thromb Vasc Biol* **28**, 1928–1936.

[34] Wang S, Xu M, Li F, Wang X, Bower KA, Frank JA, Lu Y, Chen G, Zhang Z, and Ke Z, et al (2012). Ethanol promotes mammary tumor growth and angiogenesis: the involvement of chemoattractant factor MCP-1. *Breast Cancer Res Treat* **133**, 1037–1048.

[35] Niu J, Azfer A, Zhelyabovska O, Fatma S, and Kolattukudy PE (2008). Monocyte chemotactic protein (MCP)-1 promotes angiogenesis via a novel transcription factor, MCP-1-induced protein (MCPIP). *J Biol Chem* **283**, 14542–14551.

[36] Weber KS, Nelson PJ, Gröne HJ, and Weber C (1999). Expression of CCR2 by endothelial cells: implications for MCP-1 mediated wound injury repair and in vivo inflammatory activation of endothelium. *Arterioscler Thromb Vasc Biol* **19**, 2085–2093.

[37] Salcedo R, Ponce ML, Young HA, Wasserman K, Ward JM, Kleinman HK, Oppenheim JJ, and Murphy WJ (2000). Human endothelial cells express CCR2 and respond to MCP-1: direct role of MCP-1 in angiogenesis and tumor progression. *Blood* **96**, 34–40.

[38] Garcia-Roman J and Zentella-Dehesa A (2013). Vascular permeability changes involved in tumor metastasis. *Cancer Lett* **335**, 259–269.

[39] Wilson TJ, Nannuru KC, Futakuchi M, and Singh RK (2010). Cathepsin G-mediated enhanced TGF-β signaling promotes angiogenesis via upregulation of VEGF and MCP-1. *Cancer Lett* **288**, 162–169.

[40] Nam JS, Kang MJ, Suchar AM, Shimamura T, Kohn EA, Michalowska AM, Jordan VC, Hirohashi S, and Wakefield LM (2006). Chemokine (C-C motif) ligand 2 mediates the prometastatic effect of dysadherin in human breast cancer cells. *Cancer Res* **66**, 7176–7184.

[41] Mestdagt M, Polette M, Buttice G, Noel A, Ueda A, Foidart JM, and Gilles C (2006). Transactivation of MCP-1/CCL2 by β-catenin/TCF-4 in human breast cancer cells. *Int J Cancer* **118**, 35–42.

[42] Prest SJ, Rees RC, Murdoch C, Marshall JF, Cooper PA, Bibby M, Li G, and Ali SA (1999). Chemokines induce the cellular migration of MCF-7 human breast carcinoma cells: subpopulations of tumour cells display positive and negative chemotaxis and differential in vivo growth potentials. *Clin Exp Metastasis* **17**, 389–396.

[43] Robinson SC, Scott KA, and Balkwill FR (2002). Chemokine stimulation of monocyte matrix metalloproteinase-9 requires endogenous TNF-α. *Eur J Immunol* **32**, 404–412.

[44] Soria G, Lebel-Haziv Y, Ehrlich M, Meshel T, Suez A, Avezov E, Rozenberg P, and Ben-Baruch A (2012). Mechanisms regulating the secretion of the promalignancy chemokine CCL5 by breast tumor cells: CCL5's 40s loop and intracellular glycosaminoglycans. *Neoplasia* **14**, 1–19.

[45] Proudfoot AE, Fritchley S, Borlat F, Shaw JP, Vilbois F, Zwahlen C, Trkola A, Marchant D, Clapham PR, and Wells TN (2001). The BBXB motif of RANTES is the principal site for heparin binding and controls receptor selectivity. *J Biol Chem* **276**, 10620–10626.

[46] Martin L, Blanpain C, Garnier P, Wittamer V, Parmentier M, and Vita C (2001). Structural and functional analysis of the RANTES-glycosaminoglycans interactions. *Biochemistry* **40**, 6303–6318.

[47] Proudfoot AE (2006). The biological relevance of chemokine-proteoglycan interactions. *Biochem Soc Trans* **34**, 422–426.

[48] Salanga CL and Handel TM (2011). Chemokine oligomerization and interactions with receptors and glycosaminoglycans: the role of structural dynamics in function. *Exp Cell Res* **317**, 590–601.

[49] Hol J, Küchler AM, Johansen FE, Dalhus B, Haraldsen G, and Oynebråten I (2009). Molecular requirements for sorting of the chemokine interleukin-8/CXCL8 to endothelial Weibel-Palade bodies. *J Biol Chem* **284**, 23532–23539.

[50] El Golli N, Issertial O, Rosa JP, and Briquet-Laugier V (2005). Evidence for a granule targeting sequence within platelet factor 4. *J Biol Chem* **280**, 30329–30335.

[51] Lau EK, Paavola CD, Johnson Z, Gaudry JP, Geretti E, Borlat F, Kungl AJ, Proudfoot AE, and Handel TM (2004). Identification of the glycosaminoglycan binding site of the CC chemokine, MCP-1: implications for structure and function in vivo. *J Biol Chem* **279**, 22294–22305.

[52] Chakravarty L, Rogers L, Quach T, Breckenridge S, and Kolattukudy PE (1998). Lysine 58 and histidine 66 at the C-terminal α-helix of monocyte chemoattractant protein-1 are essential for glycosaminoglycan binding. *J Biol Chem* **273**, 29641–29647.

[53] Voss MJ, Möller MF, Powe DG, Niggemann B, Zänker KS, and Entschladen F (2011). Luminal and basal-like breast cancer cells show increased migration induced by hypoxia, mediated by an autocrine mechanism. *BMC Cancer* **11**, 158.

[54] Rohl CA, Strauss CE, Misura KM, and Baker D (2004). Protein structure prediction using Rosetta. *Methods Enzymol* **383**, 66–93.

[55] Davis IW, Leaver-Fay A, Chen VB, Block JN, Kapral GJ, Wang X, Murray LW, Arendall III WB, Snoeyink J, and Richardson JS, et al (2007). MolProbity: all-atom contacts and structure validation for proteins and nucleic acids. *Nucleic Acids Res* **35**, W375–W383.

[56] Lubkowski J, Bujacz G, Boqué L, Domaille PJ, Handel TM, and Wlodawer A (1997). The structure of MCP-1 in two crystal forms provides a rare example of variable quaternary interactions. *Nat Struct Biol* **4**, 64–69.

[57] Gowda DC, Bhavanandan VP, and Davidson EA (1986). Isolation and characterization of proteoglycans secreted by normal and malignant human mammary epithelial cells. *J Biol Chem* **261**, 4926–4934.

[58] Gowda DC, Bhavanandan VP, and Davidson EA (1986). Isolation and characterization of membrane-associated proteoglycans from normal and malignant human mammary epithelial cells. *Glycoconjugate J* **3**, 55–70.

[59] Johnson Z, Proudfoot AE, and Handel TM (2005). Interaction of chemokines and glycosaminoglycans: a new twist in the regulation of chemokine function with opportunities for therapeutic intervention. *Cytokine Growth Factor Rev* **16**, 625–636.

[60] Esko JD, Stewart TE, and Taylor WH (1985). Animal cell mutants defective in glycosaminoglycan biosynthesis. *Proc Natl Acad Sci U S A* **82**, 3197–3201.

[61] Gotting C, Kuhn J, and Kleesiek K (2007). Human xylosyltransferases in health and disease. *Cell Mol Life Sci* **64**, 1498–1517.

[62] Gingis-Velitski S, Zetser A, Kaplan V, Ben-Zaken O, Cohen E, Levy-Adam F, Bashenko Y, Flugelman MY, Vlodavsky I, and Ilan N (2004). Heparanase uptake

is mediated by cell membrane heparan sulfate proteoglycans. *J Biol Chem* **279**, 44084–44092.

[63] Multhaupt HA and Couchman JR (2013). Heparan sulfate biosynthesis: methods for investigation of the heparanosome. *J Histochem Cytochem* **60**, 908–915.

[64] Nadanaka S and Kitagawa H (2008). Heparan sulphate biosynthesis and disease. *J Biochem* **144**, 7–14.

[65] Sarrazin S, Lamanna WC, and Esko JD (2011). Heparan sulfate proteoglycans. *Cold Spring Harb Perspect Biol* , 3.

[66] Hemmerich S, Paavola C, Bloom A, Bhakta S, Freedman R, Grunberger D, Krstenansky J, Lee S, McCarley D, and Mulkins M, et al (1999). Identification of residues in the monocyte chemotactic protein-1 that contact the MCP-1 receptor, CCR2. *Biochemistry* **38**, 13013–13025.

[67] Jiang Y, Valente AJ, Williamson MJ, Zhang L, and Graves DT (1990). Post-translational modification of a monocyte-specific chemoattractant synthesized by glioma, osteosarcoma, and vascular smooth muscle cells. *J Biol Chem* **265**, 18318–18321.

[68] Ruggiero P, Flati S, Di Cioccio V, Maurizi G, Macchia G, Facchin A, Anacardio R, Maras A, Lucarelli M, and Boraschi D (2003). Glycosylation enhances functional stability of the chemotactic cytokine CCL2. *Eur Cytokine Netw* **14**, 91–96.

[69] Ishii K, Yamagami S, Tanaka H, Motoki M, Suwa Y, and Endo N (1995). Full active baculovirus-expressed human monocyte chemoattractant protein 1 with the intact N-terminus. *Biochem Biophys Res Commun* **206**, 955–961.

[70] Kolset SO, Prydz K, and Pejler G (2004). Intracellular proteoglycans. *Biochem J* **379**, 217–227.

[71] Zehe C, Engling A, Wegehingel S, Schäfer T, and Nickel W (2006). Cell-surface heparan sulfate proteoglycans are essential components of the unconventional export machinery of FGF-2. *Proc Natl Acad Sci U S A* **103**, 15479–15484.

[72] Takahashi I, Noguchi N, Nata K, Yamada S, Kaneiwa T, Mizumoto S, Ikeda T, Sugihara K, Asano M, and Yoshikawa T, et al (2009). Important role of heparan sulfate in postnatal islet growth and insulin secretion. *Biochem Biophys Res Commun* **383**, 113–118.

[73] Wagner L, Yang OO, Garcia-Zepeda EA, Ge Y, Kalams SA, Walker BD, Pasternack MS, and Luster AD (1998). Beta-chemokines are released from HIV-1-specific cytolytic T-cell granules complexed to proteoglycans. *Nature* **391**, 908–911.

[74] Meen AJ, Øynebråten I, Reine TM, Duelli A, Svennevig K, Pejler G, Jenssen T, and Kolset SO (2011). Serglycin is a major proteoglycan in polarized human endothelial cells and is implicated in the secretion of the chemokine GROalpha/CXCL1. *J Biol Chem* **286**, 2636–2647.